Resonant scattering of plasma sheet electrons leading to diffuse auroral precipitation: 2. Evaluation for whistler mode chorus waves

Binbin Ni,[1] Richard M. Thorne,[1] Nigel P. Meredith,[2] Richard B. Horne,[2] and Yuri Y. Shprits[1,3]

Received 21 October 2010; revised 4 February 2011; accepted 4 March 2011; published 19 April 2011.

[1] Using the statistical wave power spectral profiles obtained from CRRES wave data within the 0000–0600 MLT sector under different levels of geomagnetic activity and a modeled latitudinal variation of wave normal angle distribution, we examine quantitatively the effects of lower band and upper band chorus on resonant diffusion of plasma sheet electrons for diffuse auroral precipitation in the inner magnetosphere. Whistler mode chorus-induced resonant scattering of plasma sheet electrons is geomagnetic activity dependent, varying from above the strong diffusion limit (timescale of an hour) during active times ($AE^* > 300$ nT) with peak wave amplitudes of >50 pT to weak scattering (timescale of a day) during quiet conditions ($AE^* < 100$ nT) with typical wave amplitudes of ≤10 pT. Chorus waves present at different magnetic latitudes make distinct contributions to the net diffusion rates of plasma sheet electrons, largely depending on the latitudinal variation of wave power. Upper band chorus is the controlling scattering process for electrons from ~100 eV to ~2 keV, and lower band chorus is most effective for precipitating the higher energy (>~2 keV) plasma sheet electrons in the inner magnetosphere. Efficient scattering by the combination of active time lower band and upper band chorus can cover a wide energy range from ~100 eV to >100 keV and a broad interval of equatorial pitch angle, thereby accounting for the formation of observed electron pancake distribution. Decreased chorus scattering during less disturbed times can also modify the magnetic local time distribution of plasma sheet electrons. Compared to the effects of chorus waves, electron cyclotron harmonic wave-induced resonant diffusion coefficients are at least 1 order of magnitude smaller and are negligible under any geomagnetic condition, indicating that chorus waves act as the major contributor dominantly responsible for diffuse auroral precipitation in the inner magnetosphere. Chorus-driven momentum diffusion and mixed diffusion are also important. Lower band and upper band chorus can cause strong momentum diffusion of plasma sheet electrons in the energy ranges of ~500 eV to ~2 keV and ~2 keV to ~3 keV, respectively, which can significantly result in energization of the electrons and attenuation of the waves.

Citation: Ni, B., R. M. Thorne, N. P. Meredith, R. B. Horne, and Y. Y. Shprits (2011), Resonant scattering of plasma sheet electrons leading to diffuse auroral precipitation: 2. Evaluation for whistler mode chorus waves, *J. Geophys. Res.*, *116*, A04219, doi:10.1029/2010JA016233.

1. Introduction

[2] It has been long agreed that diffuse aurora, which usually forms the equatorward boundary of auroral oval and considerably modifies the properties of the ionosphere and the middle atmosphere, originates from the wave-particle interaction induced precipitation of plasma sheet electrons in the energy range of ~100 eV to tens of keV. A number of magnetospheric wave modes have been proposed as viable candidates for the production of diffuse aurora through resonant wave-particle interactions. Electrostatic electron cyclotron harmonic (ECH) waves and electromagnetic whistler mode chorus waves have received the most extensive investigations [e.g., *Kennel et al.*, 1970; *Lyons*, 1974c; *Inan et al.*, 1992; *Villalón and Burke*, 1995; *Horne and Thorne*, 2000; *Horne et al.*, 2003; *Ni et al.*, 2008; *Meredith et al.*, 2000, 2009; *Su et al.*, 2009, 2010; *Thorne et al.*, 2010]. Previous studies showed that both ECH waves and chorus can

[1]Department of Atmospheric and Oceanic Sciences, University of California, Los Angeles, California, USA.
[2]British Antarctic Survey, Cambridge, UK.
[3]Institute of Geophysics and Planetary Physics, University of California, Los Angeles, California, USA.

0148-0227/11/2010JA016233

cause strong pitch angle diffusion of plasma sheet electrons under certain conditions to account for the occurrence of diffuse aurora. However, detailed quantitative evaluations of resonant diffusion of plasma sheet electrons using statistical wave information are required to fully address the relative roles of each of the above two wave modes in driving diffuse auroral precipitation under different levels of geomagnetic activity.

[3] The present work is a companion paper to *Ni et al.* [2011a] (hereafter referred to as paper 1). Paper 1 focused on ECH wave scattering of plasma sheet electrons in the inner magnetosphere (L < ~8). Using the CRRES wave database, a statistical model of the wave power spectral intensity was established for multiple harmonic ECH emissions under geomagnetically quiet, moderate, and active conditions, which were then utilized in combination with HOTRAY [*Horne*, 1989] simulation results to compute the bounce-averaged diffusion coefficients of plasma sheet electrons by ECH waves. Here, we extend the study by quantifying the effect of resonant diffusion of plasma sheet electrons due to whistler mode chorus waves and compare the results with those for ECH waves shown in paper 1 to evaluate the relative roles of each wave mode. The CRRES wave data obtained from the 0000–0600 MLT range is used to build up a statistical wave power model for chorus emissions in the inner magnetosphere over the spatial region where the diffuse aurora is most intense [*Petrinec et al.*, 1999; *Newell et al.*, 2009]. The wave model is then used to evaluate the scattering of plasma sheet electrons from 10 eV to 100 keV under different levels of geomagnetic activity.

[4] Among the most intense electromagnetic emissions in the terrestrial environment, whistler mode chorus waves are observed in the Earth's magnetosphere, predominantly in the low-density region outside the plasmasphere, over a broad range of local times (2200–1300 MLT). Chorus waves occur characteristically in two frequency bands, a lower band (0.1–0.5 f_{ce}), where f_{ce} is equatorial electron gyrofrequency) and an upper band (0.5–0.8 f_{ce}) [*Burtis and Helliwell*, 1976; *Meredith et al.*, 2001]. As coherent intermittent emissions, chorus waves consist of discrete elements or wave packets, which last on a timescale of less than one second, and show a rising or falling tone in time-frequency power spectrograms [e.g., *Nunn et al.*, 1997; *Hospodarsky et al.*, 2001; *Santolík et al.*, 2003, 2004, 2006; *Chum et al.*, 2007; *Schriver et al.*, 2010]. Chorus emissions are largely controlled by magnetic substorm activity and intensify when substorm activity is enhanced [*Meredith et al.*, 2001]. Typically, chorus amplitudes lie in the range 1–100 pT [*Burtis and Helliwell*, 1975; *Meredith et al.*, 2003; *Li et al.*, 2009a], however, amplitudes of ~1 nT or above have been reported during intense geomagnetic activity [*Parrot and Gaye*, 1994; *Cattell et al.*, 2008; *Cully et al.*, 2008].

[5] Observations also show distinct differences in the characteristics of nightside (2200–0600 MLT) chorus and dayside (0600–1300 MLT) chorus. Specifically, nightside chorus is predominantly confined to magnetic latitudes within 15° of the equator while dayside chorus can propagate to much higher latitudes due to weaker Landau damping [*Tsurutani and Smith*, 1974; *Meredith et al.*, 2001; *Horne et al.*, 2005a; *Bortnik et al.*, 2007; *Li et al.*, 2009a]. Nightside chorus also tends to propagate with wave normal angles smaller than those for dayside chorus. It has been proposed theoretically [*Bortnik et al.*, 2008a] and later confirmed observationally [*Bortnik et al.*, 2009] that dayside chorus can propagate into the plasmasphere and there evolve into the plasmaspheric hiss. In addition, while nightside chorus occurs predominantly during geomagnetically disturbed periods [e.g., *Meredith et al.*, 2003; *Li et al.*, 2009a], dayside chorus can persist even for relatively quiet conditions with the highest occurrence at $L > 7$ [*Li et al.*, 2009a]. Nightside, equatorial ($|\lambda| < 15°$, where λ is magnetic latitude) chorus waves can be excited by cyclotron resonance with anisotropic 1–100 keV electrons injected near midnight from the plasma sheet [*Kennel and Petschek*, 1966]. The excitation of nightside whistler mode chorus emissions in the low-density plasma trough was investigated in detail during the two injection events of anisotropic plasma sheet electrons into the inner magnetosphere observed by the CRRES satellite [*Li et al.*, 2008] and by the THEMIS spacecraft [*Li et al.*, 2009b], respectively. The simulated results indicated that newly injected electrons of 1 keV to 10s keV were responsible for the intensification of lower band and upper band nightside chorus during the linear growth phase. In contrast, the persistent occurrence of dayside chorus could be attributed to the natural enhancement of electron anisotropy in the noon sector in combination with solar wind driven compressions and electron injections [*Li et al.*, 2009a]. *Jordanova et al.* [2010] have coupled the RCM and RAM codes to evaluate the global distribution of excited chorus emissions, which, however, is outside the scope of this study.

[6] Nonlinear wave growth theories have also been developed to better understand the generation process and wave characteristics of chorus emissions [e.g., *Nunn et al.*, 1997, 2009; *Omura et al.*, 2008, 2009]. It is currently agreed that the nonlinear phase occurs when the linear growth of chorus waves reaches a threshold value above the background noise level. *Katoh and Omura* [2007] and *Omura et al.* [2008] simulated the nonlinear growth and saturation of parallel propagating chorus. *Omura et al.* [2009] proposed a nonlinear mechanism to explain the frequently observed gap at 0.5 f_{ce} of chorus emissions. *Nunn et al.* [2009] used a one-dimensional Vlasov hybrid simulation code to simulate the dynamical spectra (i.e., frequency-time spectrograms) and reproduced the chorus signals observed by CLUSTER. Self-consistent particle simulation of whistler mode triggered emissions was performed by *Hikishima et al.* [2010] to study the generation and saturation of whistler waves at the magnetic equator.

[7] The importance of whistler mode chorus to radiation belt electron dynamics has been recognized due to its dual role in both the acceleration and precipitation of radiation belt energetic electrons [e.g., *Horne and Thorne*, 2003; *Horne et al.*, 2005a; *Thorne et al.*, 2005a; *Albert*, 2004, 2007; *Bortnik and Thorne*, 2007; *Summers et al.*, 2007a, 2007b; *Shprits et al.*, 2008, 2009b]. Chorus can efficiently transfer energy from the abundant low-energy electron (~10–100 keV) population to higher energy electrons [e.g., *Thorne et al.*, 2005a]. Stochastic energization via gyroresonance with chorus can generate relativistic (>~1 MeV) electrons outside the plasmapause in the inner magnetosphere. There is considerable theoretical and observational evidence [e.g., *Meredith et al.*, 2002; *Reeves et al.*, 2003; *Summers et al.*, 2002, 2004; *Horne et al.*, 2005a, 2005b; *Shprits et al.*, 2006a; *Li et al.*, 2007; *Thorne et al.*, 2007] that energy diffusion due to chorus is an essential candidate for

the enhancements of energetic electron (>~100 keV) fluxes near the heart of the outer zone during storms or during periods of prolonged substorm activity. More recently, relativistic turning acceleration (RTA) and ultrarelativistic acceleration (UTA) have been proposed as very efficient energization mechanisms for electrons interacting with discrete chorus wave packet(s) in cosmic plasma environments [e.g., *Omura et al.*, 2007; *Summers and Omura*, 2007; *Furuya et al.*, 2008]. Whistler mode chorus can also cause efficient pitch angle scattering of electrons into the loss cone leading to precipitation into the atmosphere and net losses of energetic electrons from the outer radiation belt [*Lorentzen et al.*, 2001; *O'Brien et al.*, 2004; *Thorne et al.*, 2005b; *Orlova and Shprits*, 2010]. For example, *Thorne et al.* [2005b] found that chorus-driven cyclotron resonance could be responsible for the microbursts of relativistic electron precipitation observed by SAMPEX on the dayside [*O'Brien et al.*, 2004], while *Orlova and Shprits* [2010] showed that due to field line stretching on the nightside chorus waves could also explain the nightside microburst precipitation. To quantify the diffusion effects of chorus waves on radiation belt electrons in both pitch angle and energy space, numerous studies have applied quasi-linear theory which assumes that chorus waves can be represented by a weakly turbulent continuous (k, ω) spectrum and that wave induced particle scattering is stochastic and caused by a succession of small amplitude waves with random phase. Quasi-linear theory provides an effective overall description of resonant diffusion process, but it cannot incorporate phase trapping by the wavefield or highly nonlinear effects. *Karpman et al.* [1974] were among the first to study the nonlinear theory for a quasi-monochromatic whistler wave packet interacting with the resonant particles in an inhomogeneous plasma. *Albert* [2000, 2002] analyzed the nonlinear interactions between radiation belt particles and a monochromatic electromagnetic wave. A number of following studies incorporated the effect of fast frequency drift to explore the nonlinear interactions for radiation belt electron acceleration by lightning-induced whistlers [*Trakhtengerts et al.*, 2003] and by chorus wave packets [*Demekhov et al.*, 2006, 2009]. Recently, very large amplitude whistler mode chorus have been observed both by STEREO [*Cattell et al.*, 2008] and by THEMIS [*Cully et al.*, 2008], suggesting a new paradigm for the interaction between energetic electrons and chorus waves. Using a general, relativistic, oblique test particle code, *Bortnik et al.* [2008b] investigated the effect of large amplitude chorus on energetic electrons and found that above a certain critical amplitude the nature of wave-particle interaction changes qualitatively from quasi-linear diffusion processes and needs to be treated with a nonlinear approach. Although the nonlinear effects of chorus-driven particle diffusion could be significant, quasi-linear formalism has been well established and been applied extensively for evaluation of wave induced resonant scattering at radiation belt energies with remarkable effectiveness [e.g., *Lyons et al.*, 1971, 1972; *Lyons*, 1974a, 1974b; *Albert*, 1994, 2005, 2007, 2008; *Abel and Thorne*, 1998a, 1998b; *Horne et al.*, 2003, 2005a, 2005b; *Thorne et al.*, 2005a, 2005b, 2007, 2010; *Glauert and Horne*, 2005; *Summers*, 2005; *Varotsou et al.*, 2005, 2008; *Shprits et al.*, 2006b, 2007, 2008, 2009a, 2009b; *Summers et al.*, 2007a, 2007b; *Summers et al.*, 2008; *Fok et al.*, 2008; *Tao et al.*, 2008, 2009, 2011; *Shprits and Ni*, 2009; *Albert et al.*, 2009; *Xiao et al.*, 2009, 2010; *Su et al.*, 2009, 2010; *Subbotin and Shprits*, 2009; *Subbotin et al.*, 2010]. A recent study of *Albert* [2010] also demonstrated that suitably averaging the monochromatic diffusion coefficients over chorus frequency and wave normal angle parameters can favorably reproduce the full broadband quasi-linear results. Therefore, in the present study we adopt the quasi-linear equations to quantify the average properties of diffusion process by chorus waves.

[8] While the interactions between whistler mode chorus and energetic magnetospheric electrons (>~100 keV) have been well investigated, much less attention has been paid to the interactions between chorus waves and magnetospheric electrons below ~100 keV, typically plasma sheet electrons of ~100 eV to tens of keV. Oblique high-frequency chorus emissions are able to resonate with the bulk of the plasma sheet electron population [*Inan et al.*, 1992] and has a spatial (MLT, L) distribution similar to that of diffuse aurora [*Hardy et al.*, 1985; *Meredith et al.*, 2009]. By evaluating the effect of pitch angle diffusion by lower band and upper band chorus, *Inan et al.* [1992] suggested that lower band chorus could cause scattering loss of high-energy electrons (10–50 keV) often related to pulsating aurora, while upper band chorus could scatter the lower energy electrons (1–10 keV) responsible for the dominant energy input of diffuse aurora. *Villalón and Burke* [1995] also presented a test particle theory as well as numerical calculations for the interactions of whistler mode chorus with <10 keV electrons near the equatorial plasma sheet and found that upper band chorus could scatter plasma sheet electrons into the atmospheric loss cone very efficiently for the formation of diffuse aurora. More recently, *Ni et al.* [2008] performed a quantitative analysis of the resonant scattering of plasma sheet electrons at $L = 6$ using empirical wave power distributions for lower band and upper band chorus. They suggested that upper band chorus is the dominant scattering process for electrons below ~5 keV while lower band chorus is more effective at higher energies, especially near the loss cone. Furthermore, they concluded that chorus scattering could be a major contributor to the origin of diffuse aurora and should also control the MLT distribution of the injected plasma sheet electrons. The evolution of plasma sheet electron pitch angle distribution due to resonant interactions with the double-band chorus emissions was further investigated by *Su et al.* [2009] by solving the two-dimensional bounce-averaged Fokker-Planck equation with the quasi-linear diffusion coefficients computed based on a high density approximation and an assumed exponentially time-decaying model of chorus wave amplitude. *Thorne et al.* [2010] analyzed different types of VLF waves measured by CRRES at $L = 5$ under geomagnetically moderate conditions and evaluated their effects on the trapped electrons. They found that only chorus waves can explain both the rate at which electrons are scattered into the atmosphere and the distribution of trapped electrons left behind in space.

[9] Since accurate evaluations of resonant diffusion coefficients by chorus waves critically depend on the accuracy of the wave power adopted for the computations, in the present study we utilize the CRRES plasma wave database to establish the statistically reliable wave power models for both lower band and upper band chorus waves in the midnight-to-dawn sector (0000–0600 MLT) where the diffuse aurora activity is strongest. To explore how scattering by chorus waves varies under different levels of geomagnetic activity,

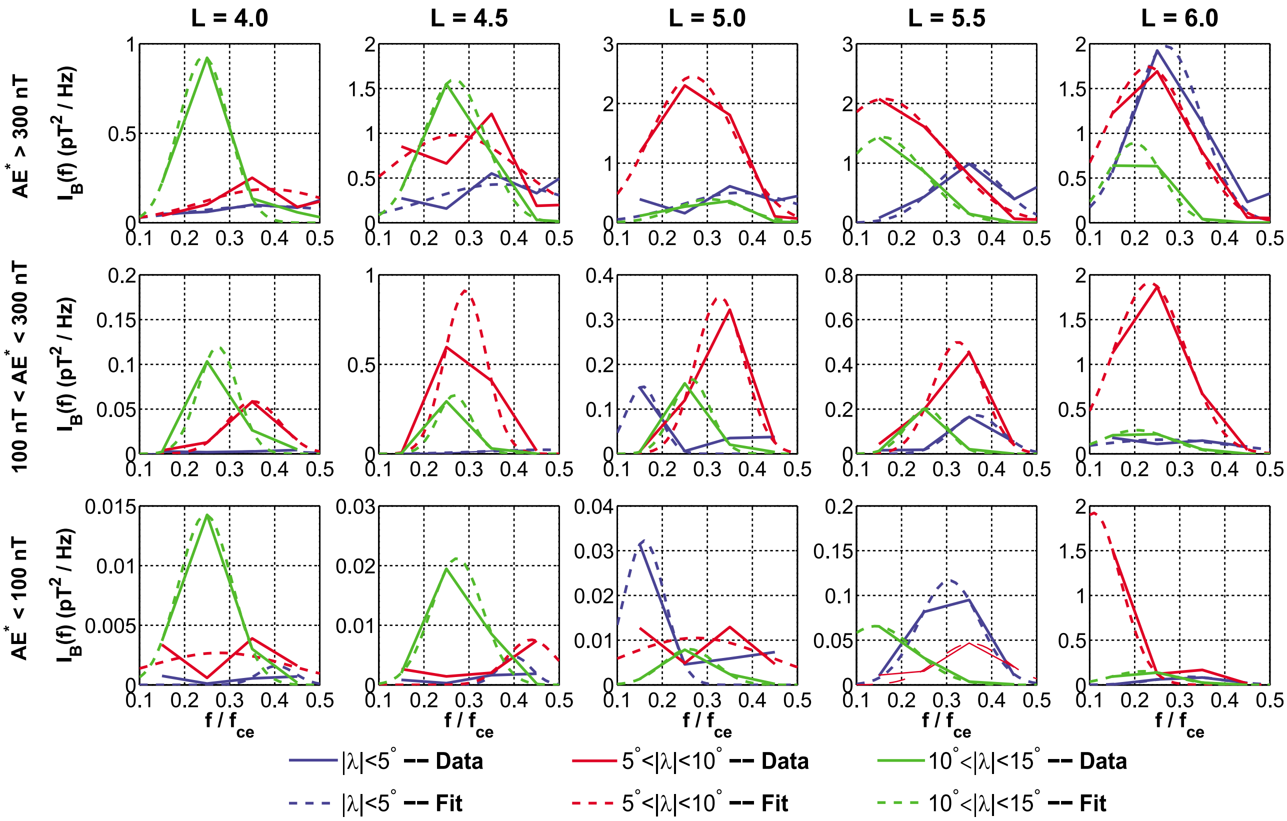

Figure 1. Averaged wave magnetic field spectral intensities (solid) at L = 4.0, 4.5, 5.0, 5.5, and 6.0 as a function of normalized wave frequency for nightside (0000–0600 MLT) lower band chorus in the three specified magnetic latitude intervals ($|\lambda| < 5°$, $5° < |\lambda| < 10°$, and $10° < |\lambda| < 15°$) under (top) active ($AE^* > 300$ nT), (middle) moderate (100 nT $< AE^* <$ 300 nT), and (bottom) quiet ($AE^* < 100$ nT) conditions. Modeled Gaussian fits to the average spectra are shown as dashed curves.

we develop a statistical model for the waves under three geomagnetic conditions: active ($AE^* > 300$ nT, where AE^* is the maximum value of the AE index in the previous 3 h), moderate (100 nT $< AE^* <$ 300 nT), and quiet ($AE^* < 100$ nT), similar to the approach used in paper 1 for ECH waves. Statistical models of wave power distribution over frequency for lower band and upper band chorus with respect to geomagnetic activity intensity are presented in section 2, together with the wave normal angle distributions established on the basis of available observations and theoretical modeling studies. A brief summary of the quasi-linear formulism for evaluation of resonant diffusion by chorus waves is presented in section 3 together with bounce-averaged diffusion rates for magnetospheric electrons in the energy range of 10 eV to 100 keV. A direct comparison is also made with the scattering rates by ECH waves under similar geomagnetic conditions. Section 4 gives a discussion of the limitation of our quasi-linear formulation to understanding diffuse auroral precipitation, together with its relevance to other ongoing studies. Finally, in section 5 we state the main conclusions of this study.

2. Chorus Wave Models

[10] Accurate calculations of quasi-linear diffusion coefficients for resonant interactions between the waves and the electrons require detailed information of the averaged wave amplitude, the wave frequency distribution, and the wave normal angle distribution.

2.1. Frequency Spectrum of Nightside Chorus Wave Power

[11] To acquire a statistically reliable frequency spectrum of chorus wave power within the 0000–0600 MLT sector we use the identical CRRES wave database constructed by *Meredith et al.* [2009]. In addition to binning the wave data as a function of half orbit (inbound and outbound) and L in steps of 0.1 L, the wave magnetic field intensities are obtained from the measured electric field intensities assuming parallel propagation [e.g., *Meredith et al.*, 2003] and are analyzed independently for lower band chorus (0.1–0.5 f_{ce}) and upper band chorus (0.5–0.8 f_{ce}) in steps of 0.1 f_{ce} for each band. Specifically, nightside lower band chorus are averaged over three separate magnetic latitude ranges, i.e., $5° < |\lambda| < 10°$, and $10° < |\lambda| < 15°$ and nightside upper band chorus are separated into two latitude ranges of $|\lambda| < 5°$ and $5° < |\lambda| < 10°$. By doing so, we construct an improved wave power model for nightside chorus and provide the opportunity to investigate the roles of chorus emissions in both pitch angle scattering and energy diffusion at different latitudes.

[12] Figure 1 shows the averaged magnetic field spectral intensities of lower band chorus ($0.1 < f/f_{ce} < 0.5$) (solid) as a function of frequency for each of the three chosen magnetic latitude intervals, from top to bottom, under active

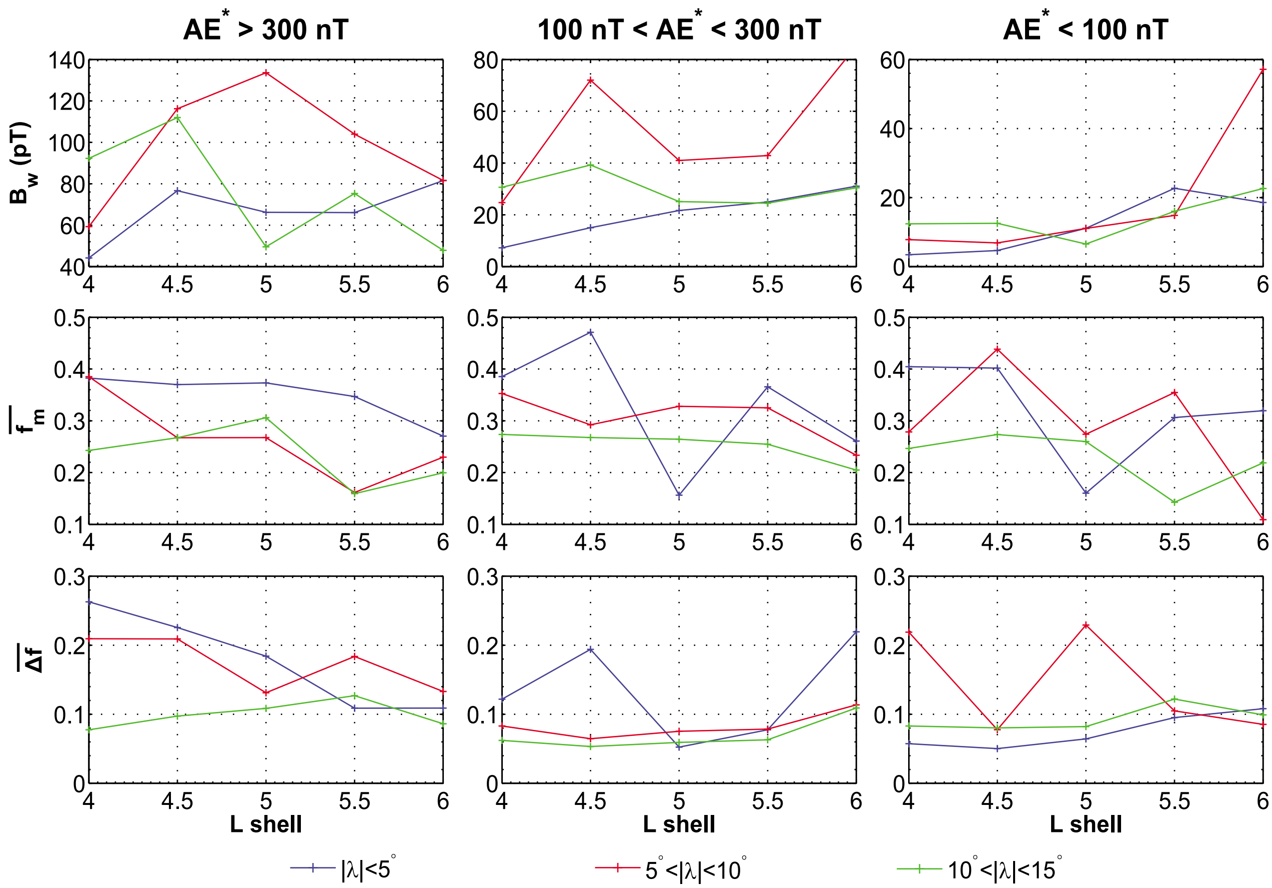

Figure 2. (top) Magnetic field amplitude, (middle) normalized peak frequency, and (bottom) normalized bandwidth obtained by applying the least squares Gaussian fit to the average spectra, as a function of L shell for nightside lower band chorus under the three geomagnetic conditions.

(AE^* > 300 nT), moderate (100 nT < AE^* < 300 nT), and quiet (AE^* < 100 nT) conditions. A least squares Gaussian fit (dashed) is also applied to the wave spectral intensity of lower band chorus at L = 4.0, 4.5, 5.0, 5.5, and 6.0. The most enhanced lower band chorus emissions are observed under active conditions (top), the wave intensities decrease slightly for moderate conditions (middle) and are much weaker by at least an order of magnitude during quiet times (bottom). Interestingly, at lower L shells (~4) lower band chorus is generally strongest at higher latitudes (10° < |λ| < 15°) and weakest near the magnetic equator (|λ| < 5°). For L = 5.0 and 5.5 lower band chorus is strongest at intermediate latitudes (5° < |λ| < 10°), while equatorial emissions (|λ| < 5°) becomes strongest for L = 6.0. Note that the exceptionally strong lower band chorus at intermediate latitudes for less disturbed geomagnetic activity (AE^* < 300 nT) may be due to the poor statistics. It is also noteworthy that lower band chorus wave intensities peak at different normalized wave frequency, depending on geomagnetic activity level, L shell location, and magnetic latitude interval.

[13] To apply the least squares Gaussian fit, we have assumed that the lower band waves have a Gaussian frequency distribution given by

$$I_B(f) = A' \exp\left[-\left(\frac{f - f_m}{\Delta f}\right)^2\right], \ (f_{lc} < f < f_{uc}) \qquad (1)$$

where I_B is the power spectral intensity of wave magnetic field (in $(\mathrm{pT})^2/\mathrm{Hz}$), f_m and Δf are the frequency of maximum wave power and bandwidth, respectively, f_{lc}(=0.1 f_{ce}) and f_{uc}(=0.5 f_{ce}) are the lower and upper cutoffs to the wave spectrum outside which the wave power is assumed to be zero, and A' is a normalization factor given by

$$A' = \frac{B_w^2}{\Delta f}\frac{2}{\pi^{1/2}}\left[\mathrm{erf}\left(\frac{f_m - f_{lc}}{\Delta f}\right) + \mathrm{erf}\left(\frac{f_{uc} - f_m}{\Delta f}\right)\right]^{-1}, \qquad (2)$$

where B_w is the wave magnetic field amplitude in units of pT and erf is the error function. The parameters obtained for the Gaussian distribution, including magnetic field amplitude (B_w), normalized peak frequency ($\overline{f_m} = f_m/f_{ce}$), and normalized bandwidth ($\overline{\Delta f} = \Delta f/f_{ce}$) for lower band chorus, are shown in Figure 2 as a function of L shell for all the three magnetic latitude intervals under the three geomagnetic conditions. The profiles of wave amplitude shown on Figure 2 (top) confirms our findings above regarding the wave power dependence on both geomagnetic activity, geocentric distance, and magnetic latitude. For instance, the average amplitude of intermediate-latitude (5° < |λ| < 10°) lower band chorus varies from more than ~100 pT during active times to well below 10 pT during quiet times, principally peaking between 4.5 and 5.5 R_E and dominating the chorus emissions at the other two magnetic latitude intervals for the cases that AE^* > 100 nT. Both equatorial (|λ| < 5°) and

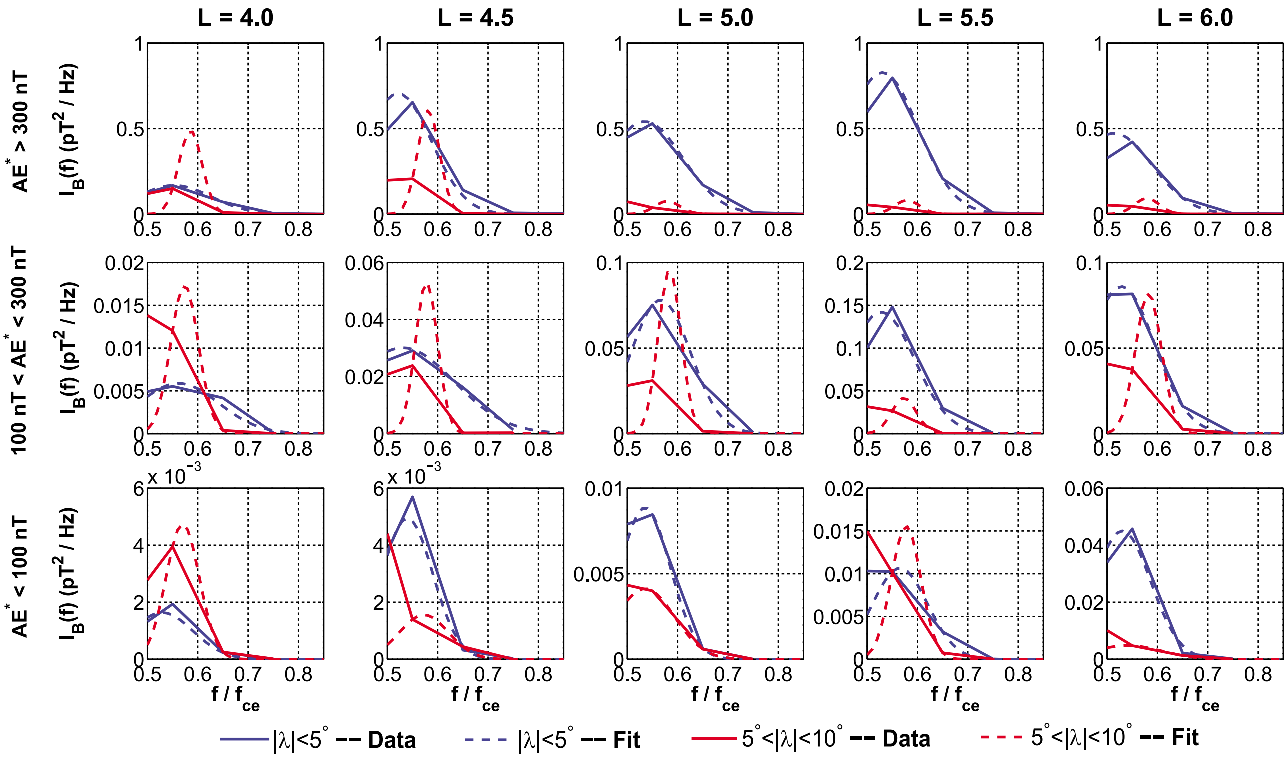

Figure 3. Averaged wave magnetic field spectral intensities (solid) at L = 4.0, 4.5, 5.0, 5.5, and 6.0 as a function of normalized wave frequency for nightside (0000–0600 MLT) upper band chorus in the two specified magnetic latitude intervals ($|\lambda| < 5°$ and $5° < |\lambda| < 10°$) under (top) active ($AE^* > 300$ nT), (middle) moderate (100 nT $< AE^* <$ 300 nT), and (bottom) quiet ($AE^* < 100$ nT) conditions. Modeled Gaussian fits to the average spectra are shown as dashed curves.

higher-latitude ($10° < |\lambda| < 15°$) lower band chorus also decrease in power with decreased intensity of geomagnetic activity and tend to become more intense than intermediate-latitude chorus during quiet times. Another feature for the frequency spectrum of nightside lower band chorus is that the peak frequency and bandwidth tend to decrease with a decrease in geomagnetic activity level but are mostly confined to 0.2–0.4 f_{ce} and 0.05–0.15 f_{ce}, respectively.

[14] A similar analysis has been performed for nightside upper band chorus as shown in Figures 3 and 4. It is evident that upper band chorus is less intense than lower band chorus under all geomagnetic conditions. Upper band chorus wave intensities are enhanced during higher levels of geomagnetic disturbance, with the averaged wave amplitude varying from ~5 pT during quiet times to >~30 pT under active conditions, and primarily peaking between L = 4.5 and 5.5. Upper band chorus is consistently most intense near the equator ($|\lambda| < 5°$) except at L = 4.0. The peak frequencies for upper band chorus vary between 0.5 and 0.6 f_{ce} and the bandwidths vary principally between 0.03 and 0.1 f_{ce}, both within a range narrower than that for lower band chorus.

[15] All the above nightside wave characteristics, except those freshly discussed here for lower band and upper band chorus, are in good agreement with the previous investigations [*Meredith et al.*, 2001, 2009]. To evaluate resonant diffusion of plasma sheet electrons, we average the model Gaussian parameters (B_w, $\overline{f_m}$, $\overline{\Delta f}$) over L = 4 to L = 6, to establish a representative frequency spectrum for both lower band and upper band chorus, which are tabulated in Table 1 for different levels of geomagnetic activity.

2.2. Wave Normal Angle Distribution of Nightside Chorus

[16] It is generally thought that generation of whistler mode chorus takes place close to the geomagnetic equatorial plane [e.g., *Burtis and Helliwell*, 1969; *Burton and Holzer*, 1974; *LeDocq et al.*, 1998]. Nightside chorus observed during geomagnetic storms is especially interesting for the investigation of the source mechanism [e.g., *Anderson and Maeda*, 1977; *Meredith et al.*, 2000]. In general, wave normal angles of whistler mode chorus detected within a few degrees of the magnetic equator are usually confined to within 20° of the magnetic field for both bands, predominantly parallel or quasi-parallel to the ambient magnetic field [*Burton and Holzer*, 1974; *Goldstein and Tsurutani*, 1984; *Santolík et al.*, 2003], in agreement with theoretical predictions [*Kennel and Thorne*, 1967]. However, as the emissions propagate away from the equatorial generation region in a nonducted mode, gradients in plasma density and magnetic field cause the average wave normal angle of both bands to increase progressively from their equatorial values, i.e., more oblique chorus propagation [*Thorne and Kennel*, 1967; *Burton and Holzer*, 1974; *Goldstein and Tsurutani*, 1984; *Breneman et al.*, 2009]. While there is some evidence of chorus excitation with an angular distribution not centered on the field direction [e.g., *Lauben et al.*, 2002; *Chum and Santolík*, 2005;

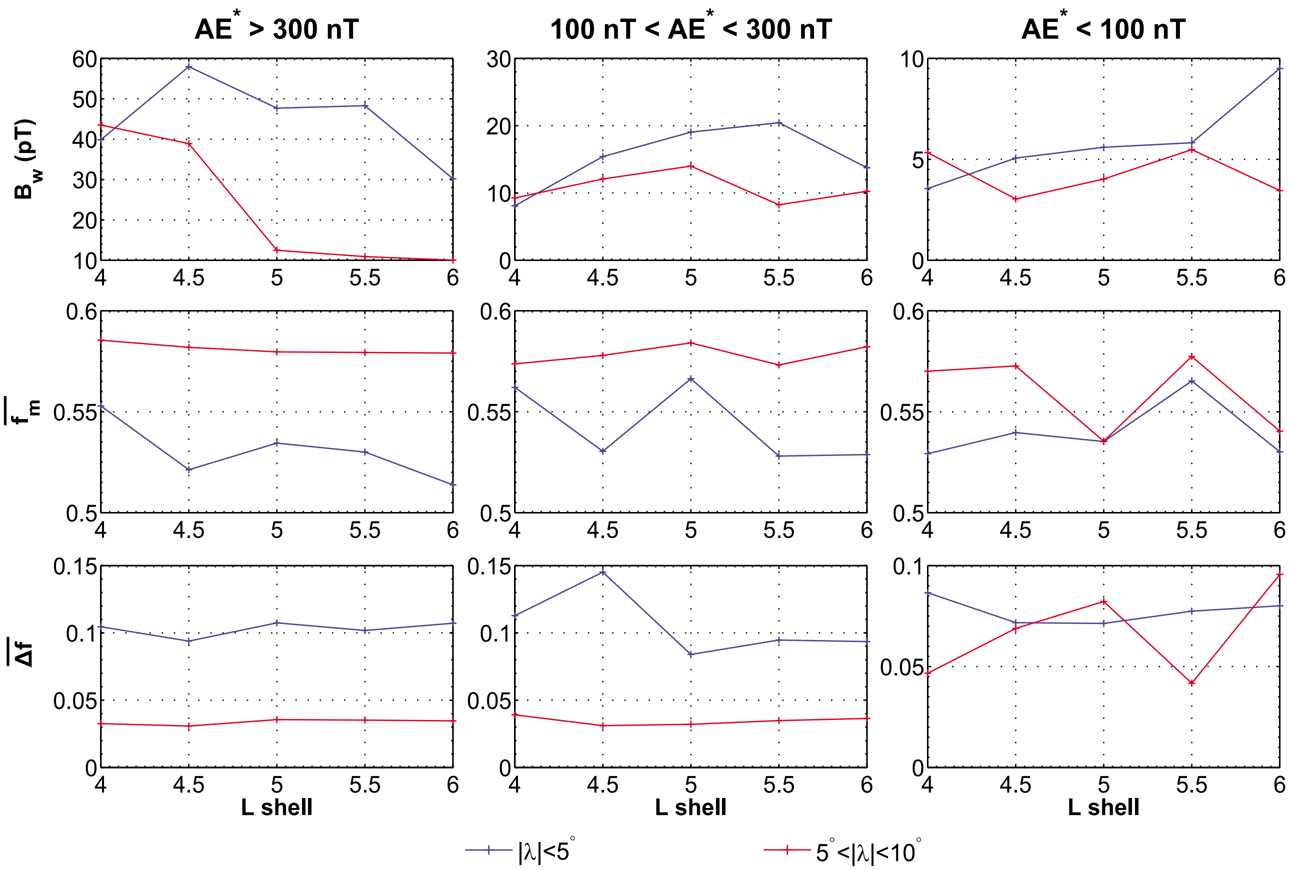

Figure 4. (top) Magnetic field amplitude, (middle) normalized peak frequency, and (bottom) normalized bandwidth obtained by applying the least squares Gaussian fit to the average spectra, as a function of *L* shell for nightside upper band chorus under the three geomagnetic conditions.

Santolík et al., 2006; *Platino et al.*, 2006], *Bortnik et al.* [2007] modeled the propagation characteristics of chorus using the statistical distributions of CRRES suprathermal electron fluxes and found that the bulk of the chorus wave power is consistent with generation in a quasi field-aligned orientation. They also showed that lower band chorus can propagate to higher latitudes than upper band chorus due to stronger Landau damping for oblique upper band chorus. Most recently, *Breneman et al.* [2009] reported chorus emission characteristics on the basis of 62 chorus events observed by the multiple CLUSTER spacecraft. In combination with a ray tracing technique, they found that the observed lower band chorus is predominantly field-aligned within a few degrees of the magnetic equator and becomes more oblique (~20°–30°) at higher latitudes, while

Table 1. Magnetic Field Amplitude B_w, Peak Normalized Wave Frequency $\overline{f_m}$ and Normalized Bandwidth $\overline{\Delta f}$[a]

	Lower Band Chorus			Upper Band Chorus	
	$\vert\lambda\vert < 5°$	$5° < \vert\lambda\vert < 10°$	$10° < \vert\lambda\vert < 15°$	$\vert\lambda\vert < 5°$	$5° < \vert\lambda\vert < 10°$
	Active Conditions (AE > 300 nT)*				
B_w (pT)	65	80	60	45	20
$\overline{f_m}$	0.35	0.3	0.25	0.53	0.58
$\overline{\Delta f}$	0.15	0.15	0.1	0.1	0.04
	Moderate Conditions (100 nT < AE < 300 nT)*				
B_w (pT)	20	35	20	15	10
$\overline{f_m}$	0.28	0.3	0.26	0.54	0.57
$\overline{\Delta f}$	0.12	0.08	0.07	0.1	0.04
	Quiet Conditions (AE < 100 nT)*				
B_w (pT)	10	10	10	5	5
$\overline{f_m}$	0.28	0.25	0.22	0.54	0.56
$\overline{\Delta f}$	0.07	0.13	0.1	0.08	0.06

[a]Obtained by applying Gaussian fits to CRRES averaged magnetic field intensities in the specified magnetic latitude intervals for nightside lower band and upper band chorus under different levels of geomagnetic activity.

Table 2. Adopted Wave Normal Angle Distributions in the Specified Magnetic Latitude Intervals for Nightside Lower Band and Upper Band Chorus

	Lower Band Chorus			Upper Band Chorus	
	$\lvert\lambda\rvert < 5°$	$5° < \lvert\lambda\rvert < 10°$	$10° < \lvert\lambda\rvert < 15°$	$\lvert\lambda\rvert < 5°$	$5° < \lvert\lambda\rvert < 10°$
θ_{lc} (deg)	0	0	0	0	0
θ_{uc} (deg)	50	50	50	45	45
θ_m (deg)	0	15	30	0	30
θ_w (deg)	30	30	30	30	30

upper band chorus tends to propagate with large wave normal angles up to their final latitudes. *Haque et al.* [2010], using the Polar data, found that for upper band chorus, wave normal angles tend to remain at or rise toward resonance cone angle for low and middle latitudes but move away from the resonance cone angle at higher latitudes due to strong Landau damping. Despite the controversies and uncertainties on the wave normal distribution of chorus emissions, in particular for upper band chorus, in the present study we use an empirical model for the wave normal angle distribution (tabulated in Table 2) which varies with magnetic latitude interval and is basically representative of the theoretical simulations and observations [e.g., *Hayakawa et al.*, 1984; *Hospodarsky et al.*, 2001; *Lauben et al.*, 2002; *Bortnik et al.*, 2006; *Li et al.*, 2008, 2009b; *Breneman et al.*, 2009; *Haque et al.*, 2010].

[17] The wave normal distribution of chorus wave power is also assumed to be Gaussian, given by

$$g(\theta) = \exp\left[-\left(\frac{\tan\theta - \tan\theta_m}{\tan\theta_w}\right)^2\right] (\theta_{lc} \le \theta \le \theta_{uc}) \qquad (3)$$

where θ is the wave normal angle, θ_m the peak, θ_w the angular width, and θ_{lc} and θ_{uc} the lower and upper bounds to the wave normal distribution outside which the wave power is zero. For simplicity, we assume that such wave normal angle distributions for both chorus bands do not change with the level of geomagnetic activity.

3. Resonant Diffusion of Plasma Sheet Electrons

[18] With the statistical information of wave power frequency spectrum and modeled wave normal angle distri-

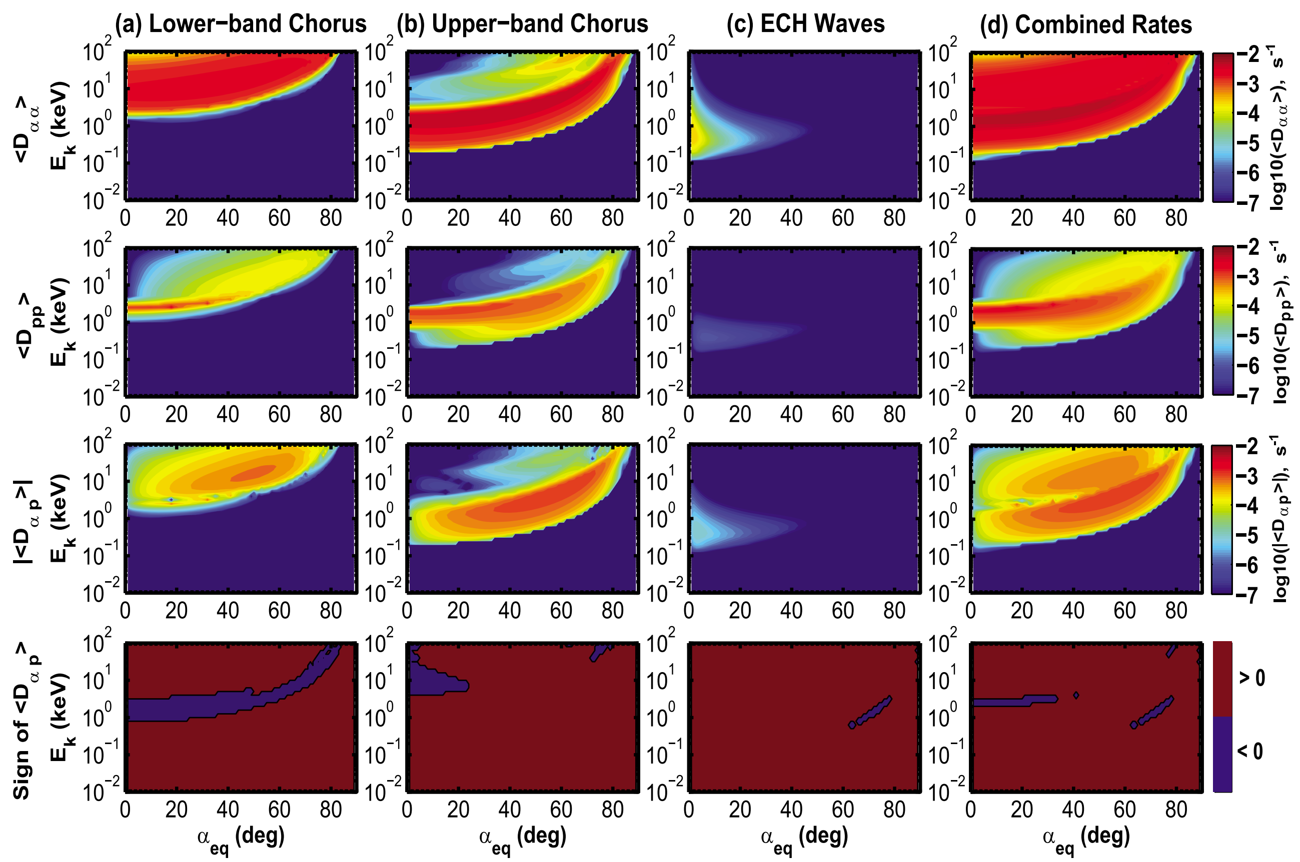

Figure 5. Bounce-averaged diffusion coefficients ($\langle D_{\alpha\alpha}\rangle$, $\langle D_{pp}\rangle$, and $\langle D_{\alpha p}\rangle$) in (equatorial pitch angle, electron kinetic energy) space for (a) lower band chorus, (b) upper band chorus, (c) ECH waves, and (d) combined diffusion at L = 6 under geomagnetically active conditions (AE* > 300 nT). The sign of mixed diffusion $\langle D_{\alpha p}\rangle$ is shown on the bottom.

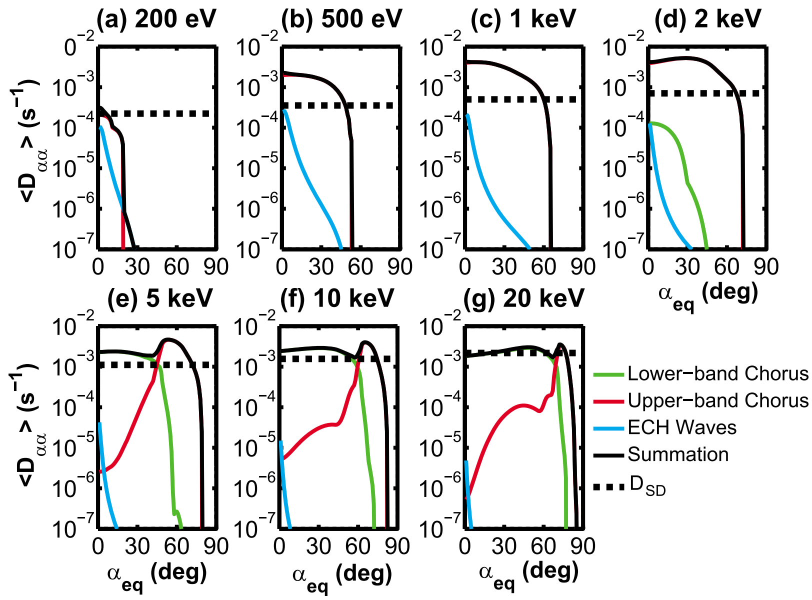

Figure 6. Bounce-averaged pitch angle scattering coefficients $\langle D_{\alpha\alpha}\rangle$ as a function of equatorial pitch angle for electrons interacting with each of the three wave modes at $L = 6$ and the net diffusion rates at the specified energies from 200 eV to 20 keV, under geomagnetically active conditions ($AE^* > 300$ nT). The horizontal dashed line in each plot represents the strong diffusion rate D_{SD} for comparison.

bution for lower band and upper band chorus developed in section 2, we use the Full Diffusion Code (FDC) [*Ni et al.*, 2008; *Shprits and Ni*, 2009] recently developed at UCLA, based on a quasi-linear formulation similar to that of *Glauert and Horne* [2005] and *Albert* [2005], to compute bounce-averaged resonant scattering rates of plasma sheet electrons by both lower band and upper band chorus under different geomagnetic conditions. Readers are referred to *Glauert and Horne* [2005] and *Albert* [2005, 2007] for elaborate equations for determination of bounce-averaged diffusion coefficients and *Ni et al.* [2008] and *Shprits and Ni* [2009] for the description of the UCLA Full Diffusion Code.

[19] Our calculations are performed at $L = 6$, including the contributions from cyclotron harmonic resonances between $N = -5$ and $N = 5$ and the Landau resonance $N = 0$. The nightside lower band chorus and upper band chorus is confined to 15° and 10° of the magnetic equator, respectively, with the assumption that the wave power distribution is constant within each specified magnetic latitude interval for both bands. The equatorial electron number density and magnetic field at $L = 6$ are the same as used for ECH waves in paper 1, obtained by averaging the CRRES observations for different geomagnetic activity levels. Specifically, the equatorial electron density is 2.88 cm^{-3}, 5.52 cm^{-3}, and 16.9 cm^{-3} and the equatorial magnetic field is 103 nT, 115 nT, and 116 nT, respectively, for geomagnetically active, moderate, and quiet conditions. Correspondingly, the ratio of equatorial electron plasma frequency to gyrofrequency is 5.3, 6.6, and 11.3. We also assume that the electron density is constant with latitude, and the magnetic field has a dipolar latitude variation scaled by the above observed equatorial values. The lower and upper cutoff frequency for lower band is 0.1 f_{ce} and 0.5 f_{ce}, and we take 0.5 f_{ce} and 0.65 f_{ce} as the lower and upper cutoff frequency for upper band chorus, since statistically there is very little wave power outside this frequency range.

[20] The net bounce-averaged coefficients for pitch angle diffusion ($\langle D_{\alpha\alpha}\rangle$), momentum diffusion ($\langle D_{pp}\rangle$) and (pitch angle, momentum) mixed diffusion ($\langle D_{\alpha p}\rangle$) by lower band chorus and upper band chorus are presented and are compared with the net diffusion rates by the multibanded ECH waves evaluated in paper 1 to obtain the combined diffusion of plasma sheet electrons by chorus and ECH waves and to differentiate the relative role of each wave mode in driving diffuse auroral precipitation.

[21] Figure 5 shows the bounce-averaged diffusion rates of electrons between 10 eV and 100 keV due to lower band chorus, upper band chorus, and ECH waves on the nightside (0000–0600 MLT) and the total diffusion rates due to combined diffusion by all three waves for geomagnetically active conditions ($AE^* > 300$ nT). Near the loss cone, lower band chorus is capable of causing efficient pitch angle scattering of electrons between 2 keV and 100 keV; upper band chorus can induce intense scattering loss of plasma sheet electrons from ~100 eV to ~3 keV. ECH waves can also cause scattering loss of plasma sheet electrons from ~100 eV to ~5 keV, but at a rate at least an order smaller than that for upper band chorus. The combined effect of pitch angle scattering by lower band chorus, upper band chorus and ECH waves, obtained under the assumption that individual wave processes are additive and independent, demonstrates that under active conditions the combination of all three waves produce rapid precipitation losses of plasma sheet electrons over a broad range of both energy and pitch angle, namely, from ~100 eV to 100 keV with equatorial pitch angle α_{eq} from the loss cone to up to ~80° depending on electron energy. A good estimate for the electron loss timescale is given by $1/\langle D_{\alpha\alpha}\rangle$ where the bounce-averaged electron pitch angle scattering rate $\langle D_{\alpha\alpha}\rangle$ is evaluated at the equatorial loss cone angle $(\alpha_{eq})_{LC}$ [e.g., *Shprits et al.*, 2006c; *Summers et al.*, 2007b; *Summers and Ni*, 2008; *Albert and Shprits*, 2009]. At $L = 6$, $(\alpha_{eq})_{LC} = 2.9°$ in a

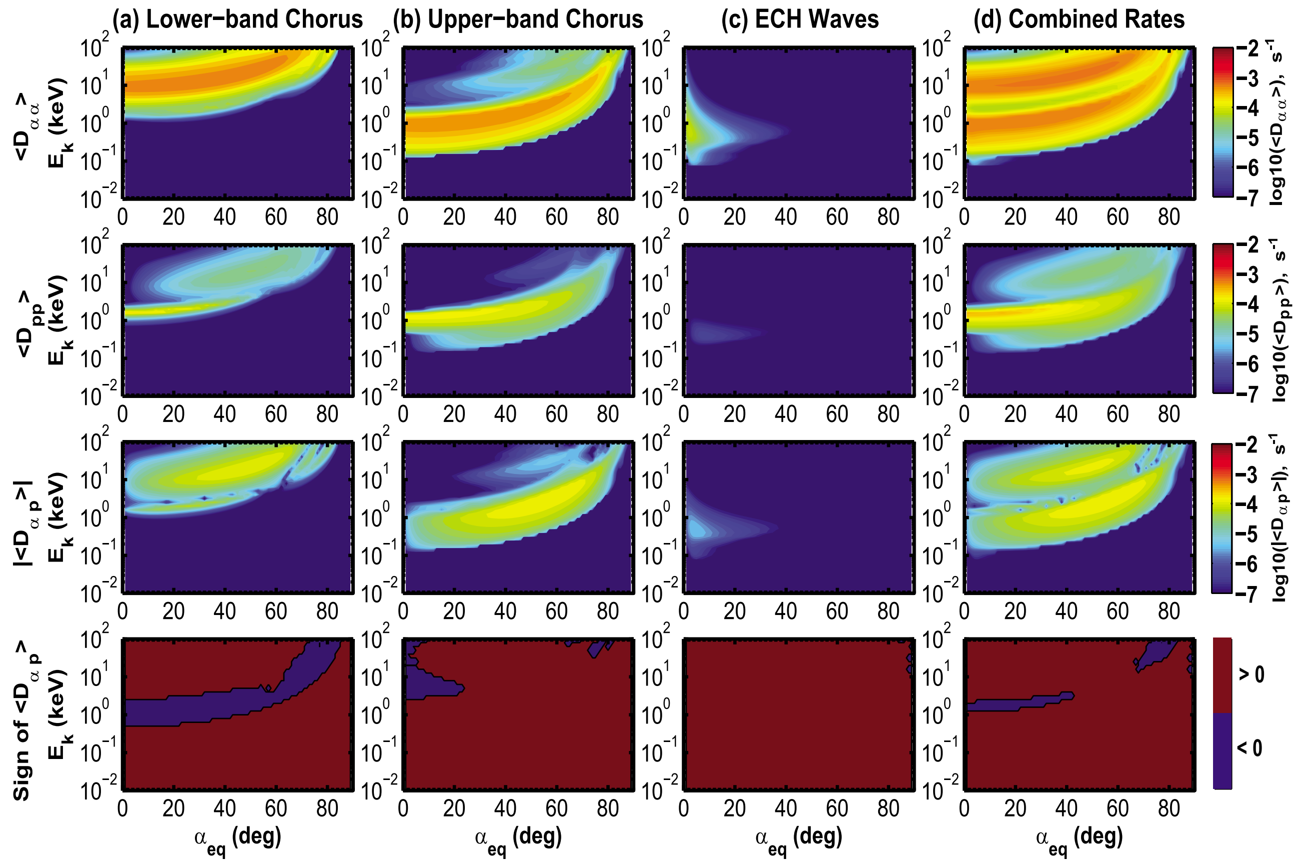

Figure 7. Same as in Figure 5, except for geomagnetically moderate conditions (100 nT < AE^* < 300 nT).

dipole field. As a consequence, we can see that during active times the majority of plasma sheet electrons (hundreds of eV to a few keV) suffer very efficient scattering loss on a timescale of less than an hour (with $\langle D_{\alpha\alpha}\rangle \approx 10^{-3}$ s^{-1} near the edge of the loss cone), shorter than their transport time for drift between midnight and dawn that generally takes several hours. Consequently, the flux of injected plasma sheet electrons will be significantly depleted during the transport process. Such intense plasma sheet electron precipitation into the atmosphere can account for the global distribution of

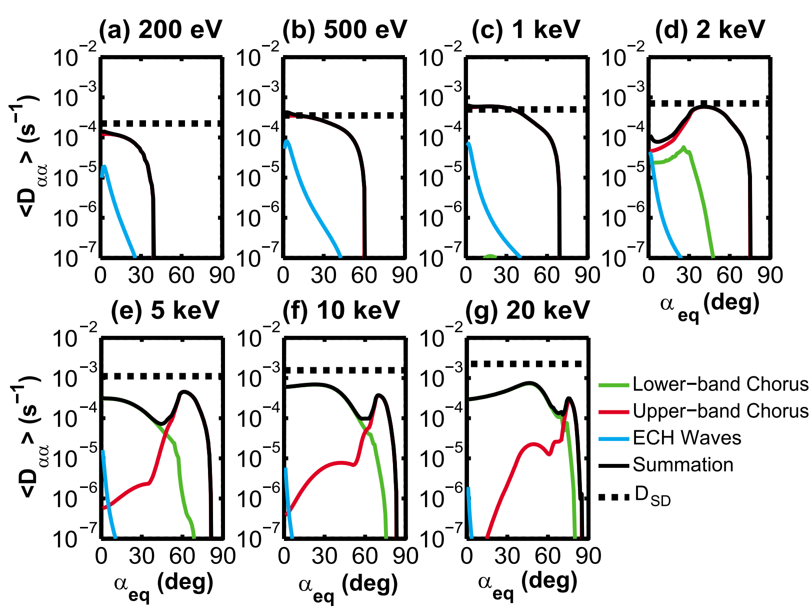

Figure 8. Same as in Figure 6, except for geomagnetically moderate conditions (100 nT < AE^* < 300 nT).

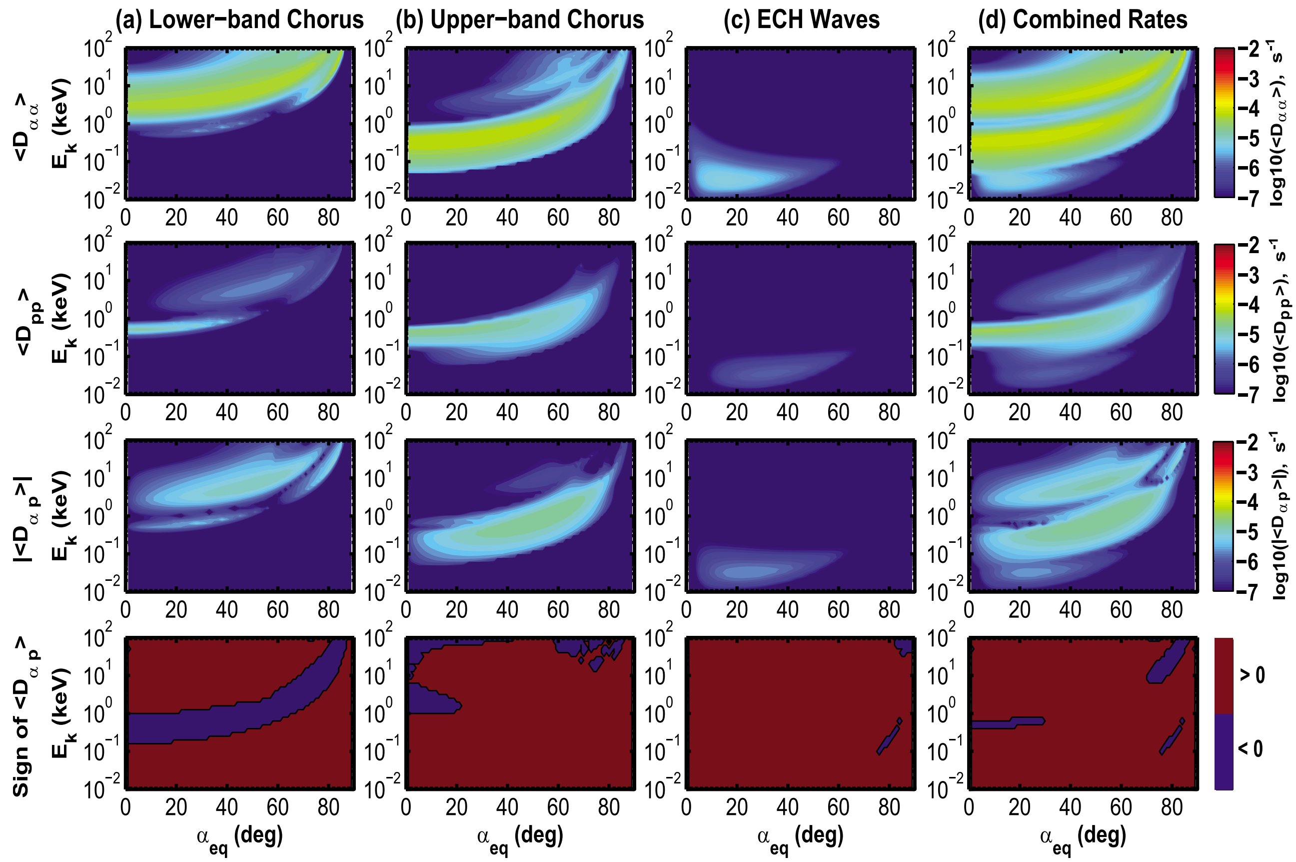

Figure 9. Same as in Figure 5, except for geomagnetically quiet conditions ($AE^* < 100$ nT).

diffuse auroral precipitation, which peaks in the post midnight sector.

[22] Our calculations also show that there is inefficient scattering of electrons with $\alpha_{eq} > \sim 80°$, which should lead to the formation of pancake shaped pitch angle distribution [e.g., *Meredith et al.*, 1999; *Su et al.*, 2009] as the injected plasma sheet electrons drift from nightside to dayside. Detailed modeling of the evolution of the injected electron distribution function is described in a companion study [*Tao et al.*, 2011]. The large rates of momentum diffusion for electrons near 1 keV by chorus waves are consistent with previous calculations of strong Landau damping of nightside chorus waves [*Bortnik et al.*, 2007]. The combined rates of mixed diffusion ($\langle D_{\alpha p} \rangle$) are generally smaller than pitch angle diffusion rates ($\langle D_{\alpha\alpha} \rangle$), though in certain ranges of electron energy and pitch angle they are comparable to each other, and should be included in modeling of the electron pitch angle distribution [e.g., *Tao et al.*, 2009; *Subbotin et al.*, 2010]. Momentum diffusion coefficients $\langle D_{pp} \rangle$ by the three wave modes show distinct features: while ECH waves have little effect on momentum diffusion, lower band chorus tends to cause most intense momentum diffusion for ~2–3 keV electrons at $\alpha_{eq} <$ 40°, and upper band chorus induces strong momentum diffusion for ~500 eV to 2 keV at lower α_{eq} and for >2 keV electrons at higher α_{eq}. The resonant electron energies for the Landau resonance with lower band and upper band chorus are consistent with the above energy ranges at lower α_{eq} where peaks of $\langle D_{pp} \rangle$ occur. *Shprits and Ni* [2009] showed that chorus-driven Landau resonance, which does not produce efficient pitch angle scattering, can result in a significant energy diffusion of 10 keV electrons at lower equatorial pitch angles. A recent study of *Ni et al.* [2011b] also found that Landau resonance dominantly accounts for the net chorus momentum diffusion rates at lower α_{eq} for ~200 eV to 3 keV electrons, regardless of the adopted magnetic field model.

[23] In principal, the results in Figure 6 for active conditions are consistent with those in Figure 4 of *Ni et al.* [2008] in that the combined rates of pitch angle scattering can approach or exceed the rate of strong diffusion [*Schulz*, 1974] (dotted horizontal lines) and in that the scattering rates exhibit similar variations with electron energy and equatorial pitch angle. However, in the present study we have adopted an improved model of chorus waves at $L = 6$ based on a statistical analysis of CRRES wave data and also included the dependence of wave power and wave normal angle distribution on magnetic latitude. Additionally, comparisons of scattering by lower band and upper band chorus with the scattering by ECH waves have been illustrated quantitatively. Due to the MLT variation of chorus wave intensity and the most intense wave activity at the nightside, it is expected that the approach to strong diffusion scattering on the nightside is not applicable at all MLTs but the net scattering loss rates can be still efficient enough to drive the precipitation loss of injected plasma sheet electrons into the atmosphere on timescales comparable to an hour.

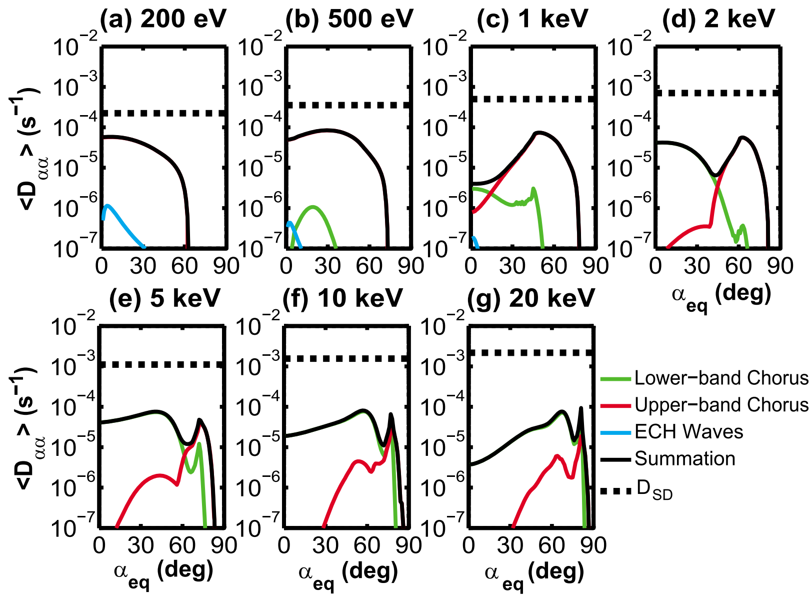

Figure 10. Same as in Figure 6, except for geomagnetically quiet conditions ($AE^* < 100$ nT).

[24] A comparison of bounce-averaged diffusion coefficients by lower band chorus, upper band chorus and ECH waves for the periods of moderate geomagnetic activity is shown in Figure 7, and a comparison of $\langle D_{\alpha\alpha}\rangle$ with the rate of strong diffusion is shown in Figure 8. Compared to the rates for active times, scattering rates are substantially smaller, mainly due to decreases in the averaged amplitudes for each wave mode. The loss timescales for diffuse auroral electrons, estimated from $\langle D_{\alpha\alpha}\rangle$ at the edge of the loss cone, are correspondingly longer on the order of an hour or more. The reduced $\langle D_{\alpha\alpha}\rangle$ near the loss cone for ~2 keV electrons could be responsible for the flattening in pitch angle distribution around a few keV [*Tao et al.*, 2011]. Upper band chorus is still capable of pitch angle scattering electrons near the loss cone at a rate comparable to that of strong diffusion at energies in the range of a few 100 eV to 1 keV. Lower band chorus can also cause rapid scattering, albeit below the strong diffusion rate, for electrons above 5 keV. However, ECH scattering is relatively insignificant. A comparison of bounce-averaged diffusion coefficients for quiet time conditions is shown in Figure 9, and $\langle D_{\alpha\alpha}\rangle$ is compared to the rate of strong diffusion in Figure 10. The combined diffusion rates under quiet time conditions are generally 2 orders of magnitude smaller than those for active time conditions, and $\langle D_{\alpha\alpha}\rangle$ is well below D_{SD}, suggesting much longer electron lifetimes of the order of hours or a day.

4. Discussions

[25] An improved statistical model of chorus waves based on the CRRES wave database has been established to compute more accurate average chorus-induced electron diffusion coefficients. However, we caution that the results of our analyses could be influenced by natural variations of plasma density and wave properties. Extremely large chorus intensities are occasionally observed [e.g., *Cully et al.*, 2008; *Cattell et al.*, 2008]. Exclusion of such extremely strong chorus wave events from the wave database used in this analysis can result in smaller averaged wave amplitude and thus weaker diffusion effects of chorus emissions on plasma sheet electrons. Variability in the magnitude of chorus wave intensity during different levels of geomagnetic activity therefore needs to be addressed in subsequent studies. On the other hand, we note that the applicability of quasi-linear theory is very likely to break down for very large amplitude whistler mode waves and for any naturally generated discrete wave packet especially with a fast frequency variation, and therefore nonlinear wave-particle scattering must be evaluated [e.g., *Karpman et al.*, 1974; *Albert*, 2000, 2002; *Trakhtengerts et al.*, 2003; *Demekhov et al.*, 2006, 2009; *Bortnik et al.*, 2008b].

[26] The wave angle distribution of chorus as a function of latitude is another important factor in the determination of quasi-linear diffusion coefficients of resonant electrons. It is generally agreed that lower band chorus waves are most probably excited close to the field-aligned direction in the source region near the magnetic equator, and subsequently become more oblique during propagation to higher latitudes. However, there is contradictory evidence on whether the generation of upper band chorus occurs in a field-aligned direction or close to the resonance cone angle. *Hayakawa et al.* [1984] and *Muto et al.* [1987], using GEOS 2 and GEOS 1 satellite observations, respectively, suggested that upper band chorus propagate with wave normal directions very close to the local resonance cone, which would imply that they are quasi-electrostatic whistler mode waves. In contrast, *Hospodarsky et al.* [2001] concluded that the waves propagate primarily parallel to the magnetic field within 5° of the magnetic equator and *Lauben et al.* [2002] concluded that the wave normal angles in the equatorial source region have values $\theta \approx 0°$. Most recently, *Haque et al.* [2010] used data from the high-frequency waveform receiver onboard the

Polar spacecraft to characterize the distribution of the chorus wave normal angle as a function of magnetic latitude. They found that for upper band chorus, wave normal angles tend to remain at or rise toward the resonance cone angle for low and middle latitudes but move away from the resonance cone angle at higher latitudes due to strong Landau damping and that for lower band chorus, wave normal angles with values $\theta < 20°$ have the highest probability of occurrence in the latitude range of 10° to 50°. Based on these previous analyses, there is clearly considerable uncertainty in the wave normal distribution of both lower band and upper band chorus and its variation with magnetic latitude. This suggests the need for a comprehensive sensitivity study of how variations in the wave normal distribution should affect chorus-induced resonant diffusion, which will be a subject of follow-up investigation.

[27] In addition, for upper band chorus we have chosen the maximum wave normal angle θ_{uc}(=45°) to be smaller than the resonance cone angle corresponding to the largest wave frequency (f/f_{ce} = 0.65 in this study). Cold plasma theory limits electromagnetic whistler mode wave propagation to angles less than resonance cone angle θ_{res}. When chorus waves propagate obliquely very close to θ_{res}, as reported [e.g., *Hayakawa et al.*, 1984; *Muto et al.*, 1987; *Haque et al.*, 2010], we need to treat the computation of chorus-driven diffusion coefficients in a more careful manner since the waves tend to be quasi-electrostatic and hot plasma theory prevails. The proximity of θ_{uc} to θ_{res} can strongly influence the quantification of resonant wave-electron interactions.

[28] To evaluate the diffusion rates by upper band chorus we have confined the wave frequency band to $0.5 < f/f_{ce} < 0.65$ on the basis of the modeled Gaussian fits to the statistically averaged CRRES wave intensities (Figure 4). There have been a number of observations showing upper band chorus occurrences with higher frequencies up to f/f_{ce} = 0.8 [*Burtis and Helliwell*, 1976; *Meredith et al.*, 2009]. The excitation mechanism for these very high frequency upper band chorus waves is an open question since the highly anisotropic distribution of source electron population required to generate these waves has been very rarely observed. While these higher frequency upper band chorus waves are observed occasionally, they generally contain much less power than the lower frequency portion of upper band chorus. Therefore, it is reasonable to adopt the upper cutoff wave frequency f_{uc}/f_{ce} = 0.65. However, it is expected that inclusion of chorus wave power at higher frequencies $f/f_{ce} > 0.65$ could lead to an increase in resonant diffusion of <~5 keV electrons and extension of diffusion rates to large equatorial pitch angles closer to 90° [*Ni et al.*, 2008], consequently influencing the occurrence of diffuse aurora and the formation of pancake distribution of plasma sheet electrons.

[29] Similar to ECH wave scattering [*Ni et al.*, 2011a], chorus-driven precipitation losses of plasma sheet electrons depend critically on the level of geomagnetic activity. Large decreases in chorus wave intensity along with decreased geomagnetic disturbances result in a dramatic drop in scattering rates at all kinetic energies and equatorial pitch angles. Slower and weaker diffuse auroral precipitation generally occurs when the geomagnetic activity is low, consistent with the previous statistical studies of the dependence of diffuse aurora intensity on the strength of geomagnetic activity [*Petrinec et al.*, 1999; *Newell et al.*, 2009]. Our results show that active time chorus activity can cause very efficient scattering of plasma sheet electrons from ~100 eV to tens of keV, approaching the regime of strong diffusion (on a timescale of an hour). Under such conditions, the bulk of the injected electrons would suffer rapid precipitation loss on a timescale shorter than the convective transport time to the dayside (approximately several hours). During geomagnetically moderate or quiet times, chorus scattering rates decrease and the precipitation rates are smaller. The dependence of the loss timescales of plasma sheet electrons on geomagnetic activity presented in this study is consistent with the conclusions of *Chen and Schulz* [2001a, 2001b] that pitch angle diffusion less than everywhere strong is needed to better simulate the global MLT distribution of diffuse auroral precipitation and also account for the observed decrease in trapped electron flux on the dayside [e.g., *Bortnik et al.*, 2007; *Li et al.*, 2010]. Also due to much stronger scattering over a broad range of pitch angle near the loss cone, the resonant diffusion by chorus shows appropriate characteristics to account for the evolution of the pancake shaped electron distribution frequently observed both at the nightside following substorm activity [*Meredith et al.*, 2000] and throughout the dayside [*Li et al.*, 2010].

[30] It is evident from our results that the role of ECH waves in inducing diffuse aurora precipitation is relatively insignificant in the inner magnetosphere, compared to that of chorus waves, which is consistent with the finding of *Thorne et al.* [2010]. Although ECH waves can separately cause efficient pitch angle scattering (on a timescale of several hours or a day) of plasma sheet electrons under geomagnetically disturbed conditions, the scattering rates are always considerably smaller than those for chorus waves, and ECH wave scattering is confined to a much smaller range of pitch angle. However, in a recent statistical study using the THEMIS filter bank wave data, *Li et al.* [2009a] found that nightside chorus waves tend to maximize at $L < 7$ and become weak or disappear at $L >$ ~8. Since the occurrence of diffuse auroral precipitation extends over a broader spatial region of $4 \le L \le 12$ [*Newell et al.*, 2009], this suggests that ECH waves, which can characteristically extend into the outer magnetosphere ~20 R_E with intense emissions (spectral density greater than >1 μV/m/Hz$^{1/2}$) occurring frequently within $L \approx 12$ [*Roeder and Koons*, 1989], could play an important or even dominant role in driving diffuse auroral precipitation in the outer ($L >$ ~8) nightside magnetosphere.

[31] *Su et al.* [2009, 2010] have also recently evaluated bounce-averaged rates of scattering by whistler mode chorus and used the results to model the evolution of plasma sheet electron pitch angle distributions following substorm injections. However, they made rather arbitrary assumption on the wave amplitudes and wave frequency spectra for both lower band and upper band chorus. They also applied a high density approximation to calculate the diffusion coefficients, which inevitably introduces errors in the diffusion rates particularly at low resonant energies [*Glauert and Horne*, 2005]. The improved wave model presented here, based on CRRES observations, and the associated diffusion coefficients should provide much more reliable

scattering rates for future modeling of the global evolution of injected plasma sheet electrons and the formation of pancake distribution.

5. Conclusions

[32] Accurate evaluation of resonant diffusion coefficients requires a realistic, detailed description of wave power, including both the wave spectral intensity as a function of frequency and the angular distribution. To investigate the importance of chorus waves in driving diffuse auroral precipitation, we have developed a statistical model of the frequency spectrum of nightside (0000–0600 MLT) chorus wave intensity under different levels of geomagnetic activity, using the high-resolution 15 month wave data provided by the Plasma Wave Experiment on board the CRRES spacecraft. We have improved the models for chorus emissions by taking into account the latitudinal variations of wave power in three magnetic latitude intervals ($|\lambda| < 5°$, $5° < |\lambda| < 10°$, and $10° < |\lambda| < 15°$) for nightside, lower band chorus and two latitude ranges ($|\lambda| < 5°$ and $5° < |\lambda| < 10°$) for nightside, upper band chorus.

[33] Using the obtained statistically improved model of chorus wave power and an empirical model of the latitudinal variations of wave normal angle distribution based on the theoretical and observations studies available, we have evaluated quantitatively the effects of lower band and upper band chorus on resonant scattering plasma sheet electrons, and their potential contributions to diffuse auroral precipitation under different levels of geomagnetic activity. The relative roles of chorus and ECH waves in driving diffuse auroral precipitation under similar levels of geomagnetic activity has also been evaluated. Our main conclusions are summarized as follows:

[34] 1. Combined scattering of plasma sheet electrons by chorus emissions and ECH waves in the inner magnetosphere can account for the occurrence and global distribution of diffuse auroral precipitation, and its variability with geomagnetic activity. However, compared to the scattering rates due to chorus waves, ECH wave scattering rates are at least 1 order of magnitude smaller and thus have a relatively negligible effect under any geomagnetic condition. Upper band chorus provides the dominant scattering process for electrons from ~100 eV to ~2 keV, while lower band chorus is most effective for precipitating higher energy (>~2 keV) plasma sheet electrons.

[35] 2. Scattering of plasma sheet electrons by whistler mode chorus strongly depends on geomagnetic activity, with strongest wave power in the inner magnetosphere under disturbed conditions. Bounce-averaged rates of pitch angle scattering near the loss cone can approach or exceed the strong diffusion limit leading to effective lifetimes (estimated by $1/\langle D_{\alpha\alpha}\rangle$ at the equatorial loss cone angle) less than or comparable to an hour during active times ($AE^* > 300$ nT), with peak chorus amplitudes of >50 pT. The scattering rates decrease to values well below the strong diffusion limit during quiet conditions ($AE^* < 100$ nT), when typical wave amplitudes are less than 10 pT.

[36] 3. Combined rates of scattering are most efficient over a broad range of pitch angle between the loss cone and a maximum pitch angle $(\alpha_{eq})_{\max}$ (between 60° and 80°), which depends on energy. Such rapid scattering for $\alpha_{eq} < (\alpha_{eq})_{\max}$ in absence of scattering above $(\alpha_{eq})_{\max}$ can lead to the development of the pancake shaped electron distribution over a time interval comparable to an hour, following the injection of plasma sheet electrons into the inner magnetosphere during substorm activity [*Tao et al.*, 2011], consistent with the observations of *Meredith et al.* [2000].

[37] 4. Rapid scattering loss of electrons on timescales (approximately hours) shorter than the transport time for convective drift to the dayside can also account for the observed [*Bortnik et al.*, 2007; *Li et al.*, 2010] MLT distribution of suprathermal electrons exterior to the plasmapause.

[38] 5. Chorus-driven momentum diffusion and mixed diffusion are smaller than pitch angle diffusion but still not negligible. In particular, lower band and upper band chorus can cause strong momentum diffusion of plasma sheet electrons in the energy range of ~500 eV to ~2 keV and ~2 keV to ~3 keV, respectively, which predominantly results from the Landau resonance between chorus waves and plasma sheet electrons and results in the energization of the electrons at intermediate pitch angles and attenuation of the waves.

[39] **Acknowledgments.** This research was supported in part by NSF grant ATM-0802843, NASA GI 08-H6I08-0117 grant, and Lab Research Fee grant 09-LR-04116720-SHPY.

[40] Robert Lysak thanks the reviewers for their assistance in evaluating this paper.

References

Abel, B., and R. Thorne (1998a), Electron scattering loss in Earth's inner magnetosphere 1. Dominant physical processes, *J. Geophys. Res.*, *103* (A2), 2385–2396, doi:10.1029/97JA02919.

Abel, B., and R. Thorne (1998b), Electron scattering loss in Earth's inner magnetosphere 2. Sensitivity to model parameters, *J. Geophys. Res.*, *103*(A2), 2397–2407, doi:10.1029/97JA02920.

Albert, J. M. (1994), Quasi-linear pitch angle diffusion coefficients: Retaining high harmonics, *J. Geophys. Res.*, *99*(A12), 23,741–23,745, doi:10.1029/94JA02345.

Albert, J. M. (2000), Gyroresonant interactions of radiation belt particles with a monochromatic electromagnetic wave, *J. Geophys. Res.*, *105*(A9), 21,191–21,209, doi:10.1029/2000JA000008.

Albert, J. M. (2002), Nonlinear interaction of outer zone electrons with VLF waves, *Geophys. Res. Lett.*, *29*(8), 1275, doi:10.1029/2001GL013941.

Albert, J. M. (2004), Using quasi-linear diffusion to model acceleration and loss from wave-particle interactions, *Space Weather*, *2*, S09S03, doi:10.1029/2004SW000069.

Albert, J. M. (2005), Evaluation of quasi-linear diffusion coefficients for whistler mode waves in a plasma with arbitrary density ratio, *J. Geophys. Res.*, *110*, A03218, doi:10.1029/2004JA010844.

Albert, J. M. (2007), Simple approximations of quasi-linear diffusion coefficients, *J. Geophys. Res.*, *112*, A12202, doi:10.1029/2007JA012551.

Albert, J. M. (2008), Efficient approximations of quasi-linear diffusion coefficients in the radiation belts, *J. Geophys. Res.*, *113*, A06208, doi:10.1029/2007JA012936.

Albert, J. M. (2010), Diffusion by one wave and by many waves, *J. Geophys. Res.*, *115*, A00F05, doi:10.1029/2009JA014732.

Albert, J. M., and Y. Y. Shprits (2009), Estimates of lifetimes against pitch angle diffusion, *J. Atmos. Sol. Terr. Phys.*, *71*, 1647–1652, doi:10.1016/j.jastp.2008.07.004.

Albert, J. M., N. P. Meredith, and R. B. Horne (2009), Three-dimensional diffusion simulation of outer radiation belt electrons during the 9 October 1990 magnetic storm, *J. Geophys. Res.*, *114*, A09214, doi:10.1029/2009JA014336.

Anderson, R. R., and K. Maeda (1977), VLF emissions associated with enhanced magnetospheric electrons, *J. Geophys. Res.*, *82*(1), 135–146, doi:10.1029/JA082i001p00135.

Bortnik, J., and R. M. Thorne (2007), The dual role of ELF/VLF chorus waves in the acceleration and precipitation of radiation belt electrons, *J. Atmos. Sol. Terr. Phys.*, *69*, 378–386, doi:10.1016/j.jastp.2006.05.030.

Bortnik, J., U. S. Inan, and T. F. Bell (2006), Landau damping and resultant unidirectional propagation of chorus waves, *Geophys. Res. Lett.*, *33*, L03102, doi:10.1029/2005GL024553.

Bortnik, J., R. M. Thorne, and N. P. Meredith (2007), Modeling the propagation characteristics of chorus using CRRES suprathermal electron fluxes, *J. Geophys. Res.*, *112*, A08204, doi:10.1029/2006JA012237.

Bortnik, J., R. M. Thorne, and N. P. Meredith (2008a), The unexpected origin of plasmaspheric hiss from discrete chorus emissions, *Nature*, *452*(7183), 62–66, doi:10.1038/nature06741.

Bortnik, J., R. M. Thorne, and U. S. Inan (2008b), Nonlinear interaction of energetic electrons with large amplitude chorus, *Geophys. Res. Lett.*, *35*, L21102, doi:10.1029/2008GL035500.

Bortnik, J., W. Li, R. M. Thorne, V. Angelopoulos, C. Cully, J. Bonnell, O. Le Contel, and A. Roux (2009), An observation linking the origin of plasmaspheric hiss to discrete chorus emissions, *Science*, *324*(5928), doi:10.1126/science.1171273.

Breneman, A. W., C. A. Kletzing, J. Pickett, J. Chum, and O. Santolik (2009), Statistics of multispacecraft observations of chorus dispersion and source location, *J. Geophys. Res.*, *114*, A06202, doi:10.1029/2008JA013549.

Burtis, W. J., and R. A. Helliwell (1969), Banded chorus: A new type of VLF radiation observed in the magnetosphere by OGO 1 and OGO 3, *J. Geophys. Res.*, *74*(11), 3002–3010, doi:10.1029/JA074i011p03002.

Burtis, W., and R. Helliwell (1975), Magnetospheric chorus: Amplitude and growth rate, *J. Geophys. Res.*, *80*(22), 3265–3270, doi:10.1029/JA080i022p03265.

Burtis, W. J., and R. A. Helliwell (1976), Magnetospheric chorus: Occurrence patterns and normalized frequency, *Planet. Space Sci.*, *24*, 1007–1010, doi:10.1016/0032-0633(76)90119-7.

Burton, R. K., and R. E. Holzer (1974), The origin and propagation of chorus in the outer magnetosphere, *J. Geophys. Res.*, *79*(7), 1014–1023, doi:10.1029/JA079i007p01014.

Cattell, C., et al. (2008), Discovery of very large amplitude whistler-mode waves in Earth's radiation belts, *Geophys. Res. Lett.*, *35*, L01105, doi:10.1029/2007GL032009.

Chen, M. W., and M. Schulz (2001a), Simulations of storm time diffuse aurora with plasmasheet electrons in strong pitch angle diffusion, *J. Geophys. Res.*, *106*(A2), 1873–1886, doi:10.1029/2000JA000161.

Chen, M. W., and M. Schulz (2001b), Simulations of diffuse aurora with plasma sheet electrons in pitch angle diffusion less than everywhere strong, *J. Geophys. Res.*, *106*(A12), 28,949–28,966, doi:10.1029/2001JA000138.

Chum, J., and O. Santolik (2005), Propagation of whistler-mode chorus to low altitudes: Divergent ray trajectories and ground accessibility, *Ann. Geophys.*, *23*, 3727–3738, doi:10.5194/angeo-23-3727-2005.

Chum, J., O. Santolík, A. W. Breneman, C. A. Kletzing, D. A. Gurnett, and J. S. Pickett (2007), Chorus source properties that produce time shifts and frequency range differences observed on different Cluster spacecraft, *J. Geophys. Res.*, *112*, A06206, doi:10.1029/2006JA012061.

Cully, C. M., J. W. Bonnell, and R. E. Ergun (2008), THEMIS observations of long-lived regions of large-amplitude whistler waves in the inner magnetosphere, *Geophys. Res. Lett.*, *35*, L17S16, doi:10.1029/2008GL033643.

Demekhov, A. G., V. Y. Trakhtengerts, M. J. Rycroft, and D. Nunn (2006), Electron acceleration in the magnetosphere by whistler-mode waves of varying frequency, *Geomagn. Aeron.*, *46*(6), 711–716, doi:10.1134/S0016793206060053.

Demekhov, A. G., V. Y. Trakhtengerts, M. J. Rycroft, and D. Nunn (2009), Efficiency of electron acceleration in the Earth's magnetosphere by whistler-mode waves, *Geomagn. Aeron.*, *49*(1), 24–29, doi:10.1134/S0016793209010034.

Fok, M.-C., R. B. Horne, N. P. Meredith, and S. A. Glauert (2008), Radiation belt environment model: Application to space weather nowcasting, *J. Geophys. Res.*, *113*, A03S08, doi:10.1029/2007JA012558.

Furuya, N., Y. Omura, and D. Summers (2008), Relativistic turning acceleration of radiation belt electrons by whistler mode chorus, *J. Geophys. Res.*, *113*, A04224, doi:10.1029/2007JA012478.

Glauert, S. A., and R. B. Horne (2005), Calculation of pitch angle and energy diffusion coefficients with the PADIE code, *J. Geophys. Res.*, *110*, A04206, doi:10.1029/2004JA010851.

Goldstein, B. E., and B. T. Tsurutani (1984), Wave normal directions of chorus near the equatorial source region, *J. Geophys. Res.*, *89*(A5), 2789–2810, doi:10.1029/JA089iA05p02789.

Haque, N., M. Spasojevic, O. Santolík, and U. S. Inan (2010), Wave normal angles of magnetospheric chorus emissions observed on the Polar spacecraft, *J. Geophys. Res.*, *115*, A00F07, doi:10.1029/2009JA014717.

Hardy, D. A., M. S. Gussenhoven, and E. Holeman (1985), A statistical model of auroral electron precipitation, *J. Geophys. Res.*, *90*(A5), 4229–4248, doi:10.1029/JA090iA05p04229.

Hayakawa, M., Y. Yamanaka, M. Parrot, and F. Lefeuvre (1984), The wave normals of magnetospheric chorus emissions observed on board GEOS 2, *J. Geophys. Res.*, *89*(A5), 2811–2821, doi:10.1029/JA089iA05p02811.

Hikishima, M., Y. Omura, and D. Summers (2010), Self-consistent particle simulation of whistler mode triggered emissions, *J. Geophys. Res.*, *115*, A12246, doi:10.1029/2010JA015860.

Horne, R. B. (1989), Path-integrated growth of electrostatic waves: The generation of terrestrial myriametric radiation, *J. Geophys. Res.*, *94*(A7), 8895–8909, doi:10.1029/JA094iA07p08895.

Horne, R. B., and R. M. Thorne (2000), Electron pitch angle diffusion by electrostatic electron cyclotron harmonic waves: The origin of pancake distributions, *J. Geophys. Res.*, *105*(A3), 5391–5402, doi:10.1029/1999JA900447.

Horne, R. B., and R. M. Thorne (2003), Relativistic electron acceleration and precipitation during resonant interactions with whistler-mode chorus, *Geophys. Res. Lett.*, *30*(10), 1527, doi:10.1029/2003GL016973.

Horne, R. B., R. M. Thorne, N. P. Meredith, and R. R. Anderson (2003), Diffuse auroral electron scattering by electron cyclotron harmonic and whistler mode waves during an isolated substorm, *J. Geophys. Res.*, *108*(A7), 1290, doi:10.1029/2002JA009736.

Horne, R. B., R. M. Thorne, S. A. Glauert, J. M. Albert, N. P. Meredith, and R. R. Anderson (2005a), Timescale for radiation belt electron acceleration by whistler mode chorus waves, *J. Geophys. Res.*, *110*, A03225, doi:10.1029/2004JA010811.

Horne, R. B., et al. (2005b), Wave acceleration of electrons in the Van Allen radiation belts, *Nature*, *437*, 227–230, doi:10.1038/nature03939.

Hospodarsky, G. B., T. F. Averkamp, W. S. Kurth, D. A. Gurnett, M. Dougherty, U. Inan, and T. Wood (2001), Wave normal and Poynting vector calculations using the Cassini radio and plasma wave instrument, *J. Geophys. Res.*, *106*(A12), 30,253–30,269, doi:10.1029/2001JA900114.

Inan, U. S., Y. T. Chiu, and G. T. Davidson (1992), Whistler-mode chorus and morningside aurorae, *Geophys. Res. Lett.*, *19*(7), 653–656, doi:10.1029/92GL00402.

Jordanova, V. K., R. M. Thorne, W. Li, and Y. Miyoshi (2010), Excitation of whistler mode chorus from global ring current simulations, *J. Geophys. Res.*, *115*, A00F10, doi:10.1029/2009JA014810.

Karpman, V. I., Y. N. Istomin, and D. R. Shklyar (1974), Nonlinear theory of a quasimonochromatic whistler mode packet in inhomogeneous plasma, *Plasma Phys.*, *16*(8), 685–703, doi:10.1088/0032-1028/16/8/001.

Katoh, Y., and Y. Omura (2007), Computer simulation of chorus wave generation in the Earth's inner magnetosphere, *Geophys. Res. Lett.*, *34*, L03102, doi:10.1029/2006GL028594.

Kennel, C. F., and H. E. Petschek (1966), Limit on stably trapped particle fluxes, *J. Geophys. Res.*, *71*(1), 1–28.

Kennel, C. F., and R. M. Thorne (1967), Unstable growth of unducted whistlers propagating at an angle to the geomagnetic field, *J. Geophys. Res.*, *72*(3), 871–878, doi:10.1029/JZ072i003p00871.

Kennel, C. F., F. L. Scarf, R. W. Fredricks, J. H. McGehee, and F. V. Coroniti (1970), VLF electric field observations in the magnetosphere, *J. Geophys. Res.*, *75*(31), 6136–6152, doi:10.1029/JA075i031p06136.

Lauben, D. S., U. S. Inan, T. F. Bell, and D. A. Gurnett (2002), Source characteristics of ELF/VLF chorus, *J. Geophys. Res.*, *107*(A12), 1429, doi:10.1029/2000JA003019.

LeDocq, M. J., D. A. Gurnett, and G. B. Hospodarsky (1998), Chorus source locations from VLF Poynting flux measurements with the Polar spacecraft, *Geophys. Res. Lett.*, *25*(21), 4063–4066, doi:10.1029/1998GL900071.

Li, W., Y. Y. Shprits, and R. M. Thorne (2007), Dynamic evolution of energetic outer zone electrons due to wave-particle interactions during storms, *J. Geophys. Res.*, *112*, A10220, doi:10.1029/2007JA012368.

Li, W., R. M. Thorne, N. P. Meredith, R. B. Horne, J. Bortnik, Y. Y. Shprits, and B. Ni (2008), Evaluation of whistler mode chorus amplification during an injection event observed on CRRES, *J. Geophys. Res.*, *113*, A09210, doi:10.1029/2008JA013129.

Li, W., R. M. Thorne, V. Angelopoulos, J. Bortnik, C. M. Cully, B. Ni, O. LeContel, A. Roux, U. Auster, and W. Magnes (2009a), Global distribution of whistler-mode chorus waves observed on the THEMIS spacecraft, *Geophys. Res. Lett.*, *36*, L09104, doi:10.1029/2009GL037595.

Li, W., R. M. Thorne, V. Angelopoulos, J. W. Bonnell, J. P. McFadden, C. W. Carlson, O. LeContel, A. Roux, K. H. Glassmeier, and H. U. Auster (2009b), Evaluation of whistler-mode chorus intensification on the nightside during an injection event observed on the THEMIS spacecraft, *J. Geophys. Res.*, *114*, A00C14, doi:10.1029/2008JA013554.

Li, W., et al. (2010), THEMIS analysis of observed equatorial electron distributions responsible for the chorus excitation, *J. Geophys. Res.*, *115*, A00F11, doi:10.1029/2009JA014845.

Lorentzen, K. R., J. B. Blake, U. S. Inan, and J. Bortnik (2001), Observations of relativistic electron microbursts in association with VLF chorus, *J. Geophys. Res.*, *106*(A4), 6017–6027, doi:10.1029/2000JA003018.

Lyons, L. R. (1974a), General relations for resonant particle diffusion in pitch angle and energy, *J. Plasma Phys.*, *12*, 45–49, doi:10.1017/S0022377800024910.

Lyons, L. R. (1974b), Pitch angle and energy diffusion coefficients from resonant interactions with ion-cyclotron and whistler waves, *J. Plasma Phys.*, *12*, 417–432, doi:10.1017/S002237780002537X.

Lyons, L. R. (1974c), Electron diffusion driven by magnetospheric electrostatic waves, *J. Geophys. Res.*, *79*(4), 575–580, doi:10.1029/JA079i004p00575.

Lyons, L. R., R. M. Thorne, and C. F. Kennel (1971), Electron pitch-angle diffusion driven by oblique whistler-mode turbulence, *J. Plasma Phys.*, *6*, 589–606, doi:10.1017/S0022377800006310.

Lyons, L. R., R. M. Thorne, and C. F. Kennel (1972), Pitch-angle diffusion of radiation belt electrons within the plasmasphere, *J. Geophys. Res.*, *77*(19), 3455–3474, doi:10.1029/JA077i019p03455.

Meredith, N. P., A. D. Johnstone, S. Szita, R. B. Horne, and R. R. Anderson (1999), "Pancake" electron distributions in the outer radiation belts, *J. Geophys. Res.*, *104*(A6), 12,431–12,444, doi:10.1029/1998JA900083.

Meredith, N. P., R. B. Horne, A. D. Johnstone, and R. R. Anderson (2000), The temporal evolution of electron distributions and associated wave activity following substorm injections in the inner magnetosphere, *J. Geophys. Res.*, *105*(A6), 12,907–12,917, doi:10.1029/2000JA900010.

Meredith, N. P., R. B. Horne, and R. R. Anderson (2001), Substorm dependence of chorus amplitudes: Implications for the acceleration of electrons to relativistic energies, *J. Geophys. Res.*, *106*(A7), 13,165–13,178, doi:10.1029/2000JA900156.

Meredith, N. P., R. B. Horne, R. H. A. Iles, R. M. Thorne, D. Heynderickx, and R. R. Anderson (2002), Outer zone relativistic electron acceleration associated with substorm-enhanced whistler mode chorus, *J. Geophys. Res.*, *107*(A7), 1144, doi:10.1029/2001JA900146.

Meredith, N. P., M. Cain, R. B. Horne, R. M. Thorne, D. Summers, and R. R. Anderson (2003), Evidence for chorus-driven electron acceleration to relativistic energies from a survey of geomagnetically disturbed periods, *J. Geophys. Res.*, *108*(A6), 1248, doi:10.1029/2002JA009764.

Meredith, N. P., R. B. Horne, R. M. Thorne, and R. R. Anderson (2009), Survey of upper band chorus and ECH waves: Implications for the diffuse aurora, *J. Geophys. Res.*, *114*, A07218, doi:10.1029/2009JA014230.

Muto, H., M. Hayakawa, M. Parrot, and F. Lefeuvre (1987), Direction finding of half-gyrofrequency VLF emissions in the off-equatorial region of the magnetosphere and their generation and propagation, *J. Geophys. Res.*, *92*(A7), 7538–7550, doi:10.1029/JA092iA07p07538.

Newell, P. T., T. Sotirelis, and S. Wing (2009), Diffuse, monoenergetic, and broadband aurora: The global precipitation budget, *J. Geophys. Res.*, *114*, A09207, doi:10.1029/2009JA014326.

Ni, B., R. M. Thorne, Y. Y. Shprits, and J. Bortnik (2008), Resonant scattering of plasma sheet electrons by whistler-mode chorus: Contribution to diffuse auroral precipitation, *Geophys. Res. Lett.*, *35*, L11106, doi:10.1029/2008GL034032.

Ni, B., R. M. Thorne, R. B. Horne, N. P. Meredith, Y. Y. Shprits, L. Chen, and W. Li (2011a), Resonant scattering of plasma sheet electrons leading to diffuse auroral precipitation: 1. Evaluation for electrostatic electron cyclotron harmonic waves, *J. Geophys. Res.*, *116*, A04218, doi:10.1029/2010JA016232.

Ni, B., R. M. Thorne, Y. Y. Shprits, K. Orlova, and N. P. Meredith (2011b), Chorus-driven resonant scattering of diffuse auroral electrons in nondipolar magnetic fields, *J. Geophys. Res.*, doi:10.1029/2011JA016453, in press.

Nunn, D., Y. Omura, H. Matsumoto, I. Nagano, and S. Yagitani (1997), The numerical simulation of VLF chorus and discrete emissions observed on the Geotail satellite using a Vlasov code, *J. Geophys. Res.*, *102*(A12), 27,083–27,097, doi:10.1029/97JA02518.

Nunn, D., O. Santolik, M. Rycroft, and V. Trakhtengerts (2009), On the numerical modeling of VLF chorus dynamical spectra, *Ann. Geophys.*, *27*, 2341–2359, doi:10.5194/angeo-27-2341-2009.

O'Brien, T. P., M. D. Looper, and J. B. Blake (2004), Quantification of relativistic electron microburst losses during the GEM storms, *Geophys. Res. Lett.*, *31*, L04802, doi:10.1029/2003GL018621.

Omura, Y., N. Furuya, and D. Summers (2007), Relativistic turning acceleration of resonant electrons by coherent whistler mode waves in a dipole magnetic field, *J. Geophys. Res.*, *112*, A06236, doi:10.1029/2006JA012243.

Omura, Y., Y. Katoh, and D. Summers (2008), Theory and simulation of the generation of whistler-mode chorus, *J. Geophys. Res.*, *113*, A04223, doi:10.1029/2007JA012622.

Omura, Y., M. Hikishima, Y. Katoh, D. Summers, and S. Yagitani (2009), Nonlinear mechanisms of lower-band and upper-band VLF chorus emissions in the magnetosphere, *J. Geophys. Res.*, *114*, A07217, doi:10.1029/2009JA014206.

Orlova, K. G., and Y. Y. Shprits (2010), Dependence of pitch-angle scattering rates and loss timescales on the magnetic field model, *Geophys. Res. Lett.*, *37*, L05105, doi:10.1029/2009GL041639.

Parrot, M., and C. A. Gaye (1994), A statistical survey of ELF waves in a geostationary orbit, *Geophys. Res. Lett.*, *21*(23), 2463–2466, doi:10.1029/94GL01700.

Petrinec, S. M., D. L. Chenette, J. Mobilia, M. A. Rinaldi, and W. L. Imhof (1999), Statistical X ray auroral emissions–PIXIE observations, *Geophys. Res. Lett.*, *26*(11), 1565–1568, doi:10.1029/1999GL900295.

Platino, M., U. S. Inan, T. F. Bell, J. S. Pickett, and P. Canu (2006), Rapidly moving sources of upper band ELF/VLF chorus near the magnetic equator, *J. Geophys. Res.*, *111*, A09218, doi:10.1029/2005JA011468.

Reeves, G. D., K. L. McAdams, R. H. W. Friedel, and T. P. O'Brien (2003), Acceleration and loss of relativistic electrons during geomagnetic storms, *Geophys. Res. Lett.*, *30*(10), 1529, doi:10.1029/2002GL016513.

Roeder, J. L., and H. C. Koons (1989), A survey of electron cyclotron waves in the magnetosphere and the diffuse auroral electron precipitation, *J. Geophys. Res.*, *94*(A3), 2529–2541, doi:10.1029/JA094iA03p02529.

Santolík, O., D. A. Gurnett, J. S. Pickett, M. Parrot, and N. Cornilleau-Wehrlin (2003), Spatio-temporal structure of storm-time chorus, *J. Geophys. Res.*, *108*(A7), 1278, doi:10.1029/2002JA009791.

Santolík, O., D. A. Gurnett, and J. S. Pickett (2004), Multipoint investigation of the source region of storm-time chorus, *Ann. Geophys.*, *22*, 2555–2563, doi:10.5194/angeo-22-2555-2004.

Santolík, O., J. Chum, M. Parrot, D. A. Gurnett, J. S. Pickett, and N. Cornilleau-Wehrlin (2006), Propagation of whistler mode chorus to low altitudes: Spacecraft observations of structured ELF hiss, *J. Geophys. Res.*, *111*, A10208, doi:10.1029/2005JA011462.

Schulz, L. (1974), Particle lifetimes in strong diffusion, *Astrophys. Space Sci.*, *31*, 37–42, doi:10.1007/BF00642599.

Schriver, D., et al. (2010), Generation of whistler mode emissions in the inner magnetosphere: An event study, *J. Geophys. Res.*, *115*, A00F17, doi:10.1029/2009JA014932.

Shprits, Y. Y., and B. Ni (2009), Dependence of the quasi-linear scattering rates on the wave normal distribution of chorus waves, *J. Geophys. Res.*, *114*, A11205, doi:10.1029/2009JA014223.

Shprits, Y. Y., R. M. Thorne, R. B. Horne, S. A. Glauert, M. Cartwright, C. T. Russell, D. N. Baker, and S. G. Kanekal (2006a), Acceleration mechanism responsible for the formation of the new radiation belt during the 2003 Halloween solar storm, *Geophys. Res. Lett.*, *33*, L05104, doi:10.1029/2005GL024256.

Shprits, Y. Y., R. M. Thorne, R. B. Horne, and D. Summers (2006b), Bounce-averaged diffusion coefficients for field-aligned chorus waves, *J. Geophys. Res.*, *111*, A10225, doi:10.1029/2006JA011725.

Shprits, Y. Y., W. Li, and R. M. Thorne (2006c), Controlling effect of the pitch angle scattering rates near the edge of the loss cone on electron lifetimes, *J. Geophys. Res.*, *111*, A12206, doi:10.1029/2006JA011758.

Shprits, Y. Y., N. P. Meredith, and R. M. Thorne (2007), Parameterization of radiation belt electron loss timescales due to interactions with chorus waves, *Geophys. Res. Lett.*, *34*, L11110, doi:10.1029/2006GL029050.

Shprits, Y. Y., D. A. Subbotin, N. P. Meredith, and S. R. Elkington (2008), Review of modeling of losses and sources of relativistic electrons in the outer radiation belts: II. local acceleration and loss, *J. Atmos. Sol. Terr. Phys.*, *70*, 1694–1713, doi:10.1016/j.jastp.2008.06.014.

Shprits, Y. Y., L. Chen, and R. M. Thorne (2009a), Simulations of pitch angle scattering of relativistic electrons with MLT-dependent diffusion coefficients, *J. Geophys. Res.*, *114*, A03219, doi:10.1029/2008JA013695.

Shprits, Y. Y., D. Subbotin, and B. Ni (2009b), Evolution of electron fluxes in the outer radiation belt computed with the VERB code, *J. Geophys. Res.*, *114*, A11209, doi:10.1029/2008JA013784.

Su, Z., H. Zheng, and S. Wang (2009), Evolution of electron pitch angle distribution due to interactions with whistler mode chorus following substorm injections, *J. Geophys. Res.*, *114*, A08202, doi:10.1029/2009JA014269.

Su, Z., H. Zheng, and S. Wang (2010), A parametric study on the diffuse auroral precipitation by resonant interaction with whistler-mode chorus, *J. Geophys. Res.*, *115*, A05219, doi:10.1029/2009JA014759.

Subbotin, D. A., and Y. Y. Shprits (2009), Three-dimensional modeling of the radiation belts using the Versatile Electron Radiation Belt (VERB) code, *Space Weather*, *7*, S10001, doi:10.1029/2008SW000452.

Subbotin, D., Y. Shprits, and B. Ni (2010), Three-dimensional VERB radiation belt simulations including mixed diffusion, *J. Geophys. Res.*, *115*, A03205, doi:10.1029/2009JA015070.

Summers, D. (2005), Quasi-linear diffusion coefficients for field-aligned electromagnetic waves with applications to the magnetosphere, *J. Geophys. Res.*, *110*, A08213, doi:10.1029/2005JA011159.

Summers, D., and B. Ni (2008), Effects of latitudinal distributions of particle density and wave power on cyclotron resonant diffusion rates of radiation belt electrons, *Earth Planets Space*, *60*, 763–771.

Summers, D., and Y. Omura (2007), Ultra-relativistic acceleration of electrons in planetary magnetospheres, *Geophys. Res. Lett.*, *34*, L24205, doi:10.1029/2007GL032226.

Summers, D., C. Ma, N. P. Meredith, R. B. Horne, R. M. Thorne, D. Heynderickx, and R. R. Anderson (2002), Model of the energization of outer-zone electrons by whistler-mode chorus during the October 9, 1990 geomagnetic storm, *Geophys. Res. Lett.*, *29*(24), 2174, doi:10.1029/2002GL016039.

Summers, D., C. Ma, N. P. Meredith, R. B. Horne, R. M. Thorne, and R. R. Anderson (2004), Modeling outer-zone relativistic electron response to whistler-mode chorus activity during substorms, *J. Atmos. Sol. Terr. Phys.*, *66*, 133–146, doi:10.1016/j.jastp.2003.09.013.

Summers, D., B. Ni, and N. P. Meredith (2007a), Timescales for radiation belt electron acceleration and loss due to resonant wave-particle interactions: 1. Theory, *J. Geophys. Res.*, *112*, A04206, doi:10.1029/2006JA011801.

Summers, D., B. Ni, and N. P. Meredith (2007b), Timescales for radiation belt electron acceleration and loss due to resonant wave-particle interactions: 2. Evaluation for VLF chorus, ELF hiss, and electromagnetic ion cyclotron waves, *J. Geophys. Res.*, *112*, A04207, doi:10.1029/2006JA011993.

Summers, D., B. Ni, N. P. Meredith, R. B. Horne, R. M. Thorne, M. B. Moldwin, and R. R. Anderson (2008), Electron scattering by whistler-mode ELF hiss in plasmaspheric plumes, *J. Geophys. Res.*, *113*, A04219, doi:10.1029/2007JA012678.

Tao, X., A. A. Chan, J. M. Albert, and J. A. Miller (2008), Stochastic modeling of multidimensional diffusion in the radiation belts, *J. Geophys. Res.*, *113*, A07212, doi:10.1029/2007JA012985.

Tao, X., J. M. Albert, and A. A. Chan (2009), Numerical modeling of multidimensional diffusion in the radiation belts using layer methods, *J. Geophys. Res.*, *114*, A02215, doi:10.1029/2008JA013826.

Tao, X., R. M. Thorne, W. Li, B. Ni, N. P. Meredith, and R. B. Horne (2011), Evolution of electron pitch-angle distributions following injection from the plasmasheet, *J. Geophys. Res.*, doi:10.1029/2010JA016245, in press.

Thorne, R. M., and C. F. Kennel (1967), Quasi-trapped VLF propagation in the outer magnetosphere, *J. Geophys. Res.*, *72*(3), 857–870, doi:10.1029/JZ072i003p00857.

Thorne, R. M., R. B. Horne, S. A. Glauert, N. P. Meredith, Y. Shprits, D. Summers, and R. R. Anderson (2005a), The influence of wave-particle interactions on relativistic electron dynamics during storms, in *Inner Magnetosphere Interactions: New Perspectives From Imaging*, *Geophys. Monogr. Ser.*, vol. 159, edited by J. Burch, M. Schulz, and H. Spence, pp. 101–112, AGU, Washington, D. C.

Thorne, R. M., T. P. O'Brien, Y. Y. Shprits, D. Summers, and R. B. Horne (2005b), Timescale for MeV electron microburst loss during geomagnetic storms, *J. Geophys. Res.*, *110*, A09202, doi:10.1029/2004JA010882.

Thorne, R. M., Y. Y. Shprits, N. P. Meredith, R. B. Horne, W. Li, and L. R. Lyons (2007), Refilling of the slot region between the inner and outer electron radiation belts during geomagnetic storms, *J. Geophys. Res.*, *112*, A06203, doi:10.1029/2006JA012176.

Thorne, R. M., B. Ni, X. Tao, R. B. Horne, and N. P. Meredith (2010), Scattering by chorus waves as the dominant cause of diffuse auroral precipitation, *Nature*, *467*, 943–946, doi:10.1038/nature09467.

Trakhtengerts, V. Y., M. J. Rycroft, D. Nunn, and A. G. Demekhov (2003), Cyclotron acceleration of radiation belt electrons by whistlers, *J. Geophys. Res.*, *108*(A3), 1138, doi:10.1029/2002JA009559.

Tsurutani, B. T., and E. J. Smith (1974), Postmidnight chorus: A substorm phenomenon, *J. Geophys. Res.*, *79*(1), 118–127, doi:10.1029/JA079i001p00118.

Varotsou, A., D. Boscher, S. Bourdarie, R. B. Horne, S. A. Glauert, and N. P. Meredith (2005), Simulation of the outer radiation belt electrons near geosynchronous orbit including both radial diffusion and resonant interaction with whistler-mode chorus waves, *Geophys. Res. Lett.*, *32*, L19106, doi:10.1029/2005GL023282.

Varotsou, A., D. Boscher, S. Bourdarie, R. B. Horne, N. P. Meredith, S. A. Glauert, and R. H. Friedel (2008), Three-dimensional test simulations of the outer radiation belt electron dynamics including electron-chorus resonant interactions, *J. Geophys. Res.*, *113*, A12212, doi:10.1029/2007JA012862.

Villalón, E., and W. J. Burke (1995), Pitch angle scattering of diffuse auroral electrons by whistler mode waves, *J. Geophys. Res.*, *100*(A10), 19,361–19,369, doi:10.1029/95JA01161.

Xiao, F., Z. Su, H. Zheng, and S. Wang (2009), Modeling of outer radiation belt electrons by multidimensional diffusion process, *J. Geophys. Res.*, *114*, A03201, doi:10.1029/2008JA013580.

Xiao, F., Z. Su, H. Zheng, and S. Wang (2010), Three-dimensional simulations of outer radiation belt electron dynamics including cross-diffusion terms, *J. Geophys. Res.*, *115*, A05216, doi:10.1029/2009JA014541.

B. Ni, Y. Y. Shprits, and R. M. Thorne, Department of Atmospheric and Oceanic Sciences, University of California, 405 Hilgard Ave., Box 951565, 7127 Math Science Bldg, Los Angeles, CA 90095-1565, USA. (bbni@atmos.ucla.edu)

R. B. Horne and N. P. Meredith, British Antarctic Survey, High Cross, Madingley Road, Cambridge CB3 0ET, UK.